NUCLEAR ORGANIZATION OF MOUSE HOX CLUSTER PARALOGS DURING MOUSE EMBRYONIC STEM CELL DIFFERENTIATION TO NEURAL STEM CELL

By

PRIYA PANICKER

A Thesis submitted to

The Graduate School of New Brunswick

Rutgers, The State University of New Jersey

And

The Graduate School of Biomedical Sciences

University of Medicine and Dentistry of New Jersey

In partial fulfillment of the requirements for the degree of

Master of Science

Graduate Program in Biomedical Engineering

Written under the direction of

Dr. Jay Tischfield

And approved by

_____

_____

_____

New Brunswick New Jersey

October 2009

Abstract of the Thesis

"Nuclear organization of mouse HOX cluster paralogs during mouse embryonic stem cell differentiation to neural stem cell"

By

Priya Panicker

Thesis Director

Dr. Jay Tischfield

In this project we use Hox genes as a genetic tool to understand how nuclear architecture regulates cell differentiation during embryonic development. Hox genes come under the category of homeobox genes, a highly evolutionarily conserved group of genes with an important role during embryogenesis. Hox genes are located on 4 distinct chromosomes, in cluster paralogs (HOX A, B, C, D). Each individual cluster contains up to 13 homologous genes and corresponding genes on different clusters (e.g., HoxA13, HoxD13) exhibit varying degrees of functional redundancy. The position of a gene in the cluster is related to its spatiotemporal pattern of expression along the anterior-posterior axis of the embryo. The coordination of the spatiotemporal expression of equivalent paralog group genes on different clusters/chromosomes is coordinated is still not known. **Our primary hypothesis is that nuclear architecture defines a regulatory framework of Hox cluster loci in the nucleus when the Hox cluster transcription is activated and maintained.** We did a comparative analysis on the Hox cluster nuclear architecture in mouse embryonic stem cells (ESCs) and fibroblast growth factors (FGF) - induced differentiation to neural stem cells (NSC). We show for the first time that Hox gene expression is induced by FGF treatment *in vitro* simultaneously in the four Hox cluster. Using three-dimensional confocal fluorescence microscopy, FISH and

computational techniques, we mapped the position of Hox gene cluster paralogs in individual nuclei of both cell types. We did not observe nuclear colocalization of Hox heterologous cluster in NSC. However, we observe that heterologous clusters tend to occupy similar nuclear domains in NSC, which may favor undetected long-range gene interactions. Nevertheless, our results indicate that Hox gene cluster nuclear three-dimensional organization is neither random nor correlated to the changes in nuclear volume and shape that parallel cell differentiation.

ACKNOWLEDGEMENTS:

I would like to express my sincere gratitude to my Principal advisor Dr.Jay Tischfield for his constant support and guidance towards helping me achieve my academic goals. I sincerely thank him for believing in my abilities and keeping me motivated to stay on track.

I also extend my gratitude to Dr.Lourdes Serrano for her whole hearted support in every step of my research work. Her excellent guidance and constant inspiration are the main reasons that I am able to accomplish this project completion.

I am thankfull to Dr. David Shreiber for his valuable time and advice in the aspect of mathematical modeling used in this research. I also extend my gratitude to Dr.Noriko Goldsmith,Dr.Irina Tereshchenko and Dr.Amrik Sahota for their valuable suggestions.

I would also like to thank my colleague Mr. Mike Wininger for his support and suggestions. I also extend my gratitude to Dr.Troy Shinbrot and Barbara Sirman their valuable suggestions. I am also thankfull to friends and labmates especially Evangeline Tzatzalos, Vamsi Rani and Yiming Chang for their support towards my research and learning.

I would like to thank my parents, my husband Manoj and son Saikrishna for enduring love and support. I am especially thankful to my 6 year old son who had been very patient with me during my graduate life with late lab hours and crazy schedules. Above all, I am as always indebted to Almighty for His grace without which I would not have achieved anything in my personal or professional life.

Table of Contents Page numbers

List of Illustrations: **Page numbers**

Section 1: INTRODUCTION

There are numerous questions arising after the completion of the decoding of the human genome sequence. It is a challenge to interpret and utilize the information originated from the human genome project to understand the most intriguing aspect of human body….the cell.

Genomes have their individual identity specified by their primary sequence. However the functionality of the genome incorporates a multifaceted regulation beyond their DNA sequence. The regulatory framework for gene expression comprises a complex hierarchical network, beginning from epigenetic chemical modification of chromatin which constitutes the basic structural unit of chromosomes, to the spatial arrangement of chromatin in the interphase nucleus. This higher order arrangement is known as nuclear architecture (Van et al, 2003). Epigenetics covers a unique field of genetics where the gene function changes without affecting its DNA sequence. Epigenetic modification of chromatin is in part achieved by DNA along with histone proteins chemical alterations, known as chromatin remodeling. DNA epigenetic modifications are primarily by methylation. Post translational modification of histones includes acetylation, methylation, phosphorylation and sumolyation (Huang et al, 2007).

Chromatin remodeling plays a key role in balancing between transcription gene activation and gene silencing (Grewal et al,2007). In addition, the level of chromatin condensation regulates the access of transcription factors and other regulatory proteins to DNA helping to maintain a cell type-specific pattern of transcriptionally active and repressed chromatin domains (Bernstein et al, 2007; Baylin et al,2007; Moon et al, 2005). Moreover, the architectural organization of the genome inside the nucleus also plays a pivotal role in the regulation of gene expression as an upper level regulatory mechanism of genome function. The concept was first introduced in 1985 by Blobel who initiated the idea that discrete 3-D structures

with respective characteristic for a given differentiated state develop from an omnipotent 3-D structure of the zygotic genome. However, we still do not understand the details of the structure to confirm or deny this hypothesis. That shows the complexity and the challenges in understanding the structural dynamics of the nucleus of the cell.

The genome is a poly-dimensional entity encompassing linear DNA with hierarchical folding leading to higher order structures. The way in which DNA is arranged in the limited space of the cell nucleus along with other nuclear components and how this fact influences gene expression is still a billion dollar question. Molecular crowding in the nucleus causes nuclear compartmentalization (Misteli et al, 2001). This suggests that DNA processes such as DNA transcription and replication are affected by molecular crowding which leads to its compartmentalization (Minton et al,2005; Marenduzzo et al,2006). Indeed, it has been shown that DNA transcription, repair and replication occur in particular compartments of the nucleus due to self organization (Misteli et al,2001). All processes occur in highly dynamic steady-state structures. The formation of the functional compartments is entirely dependent on their respective functions. Examples of self-organizing also apply to other nuclear structures such as nucleoli, Cajal bodies, PML bodies, and splicing-factor speckles. All of these organelles share a high degree of dynamic protein exchange and stochastically recruit factors from the nucleoplasm, which is reminiscent of the dynamic behavior of transcription, replication, and repair sites(Misteli et al, 2001).

Chromatin is also compartmentalized in the interphase nucleus as chromosomes in interphase cells occupy distinct, non-overlapping territories called chromosome territories (CT). The spatial nuclear arrangement of CT is still controversial. The chromosome positioning with respect to the nuclear center and periphery of the cell nucleus can be summed up under radial distribution. Radial CT distribution changes during the cell cycle and its conservation from

mother to daughter cells is still not clear. The radial distribution of CT is believed to be influenced by chromosome gene density (gene rich and gene poor chromosomes) and by the size of the chromosome. Gene rich- CTs are located towards the center of the nucleus versus gene-poor CT close to the nuclear envelope or periphery (Cremer et al, 2006; Cremer et al, 2001; Chubb et al, 2002; Meaburn et al, 2007). It is not yet clear whether cells have cell type-specific CT neighborhoods and also the extent of interaction between CT (Branco et al, 2007; Branco et al, 2006; Chubb et al, 2002).

Additionally, sub-chromosomal regions are also spatially organized inside the nucleus. Individual chromatin domains that share a common transcriptional status, also share specific pattern of epigenetic modification forming chromatin domains (Bernstein et al, 2005). It is believed that specific chromatin domains and specific genes are located in specific nuclear compartments depending of their transcriptional status (Misteli et al, 2004). Indeed, the nuclear positioning of a functionally related group of genes has been shown to differ between cell types in which expression of these genes changes (Williams et al, 2002). Moreover, a particular phenotype may require the physical interaction of genes located from very remote parts of the genome. It has been shown that long-distance chromosomal interactions can mediate gene activation or repression (Lomvardas et al, 2006). Therefore, it will be important to map long-range chromosome contacts systematically to understand how frequently they affect gene expression. It will also be crucial to study whether these contacts are the cause or the effect of regulation of gene transcription.

In this project we use Hox genes as a genetic tool to understand how nuclear architecture regulates cell differentiation during embryonic development. Hox genes are homeobox genes, a highly evolutionarily conserved group of genes with an important role during embryogenesis. Hox genes uniquely contribute to the anteroposterior (AP) patterning of the

axial skeleton of the embryo defining the body plan of vertebrates. They were first identified in Drosophila (Lewis et al, 1978). Since then, they have been found to be conserved throughout vertebrate evolution, suggesting their importance in patterning the vertebrate body plan (Deschamps et al, 2005). Hox genes are organized in clusters. Flies have eight Hox genes located in a single cluster; mammals have 39 Hox genes arranged in four clusters (A to D). It is believed that during evolution these clusters were originated as a result of duplication and divergence from one ancestor homeobox gene (Fig.1). In mammals, each cluster is approximately 120 kilo bases and holds up to 13 homologous genes (e.g. HoxA1,..,HoxA13). Each cluster is located on a different chromosome (Hox A on Chromosome 6, Hox B on Chromosome 11, Hox C on Chromosome 15, Hox D on Chromosome2). Genes that occupy the same position within a cluster on different chromosomes are called paralog genes (e.g. Hox A1, Hox B1, Hox C1 and Hox D1).

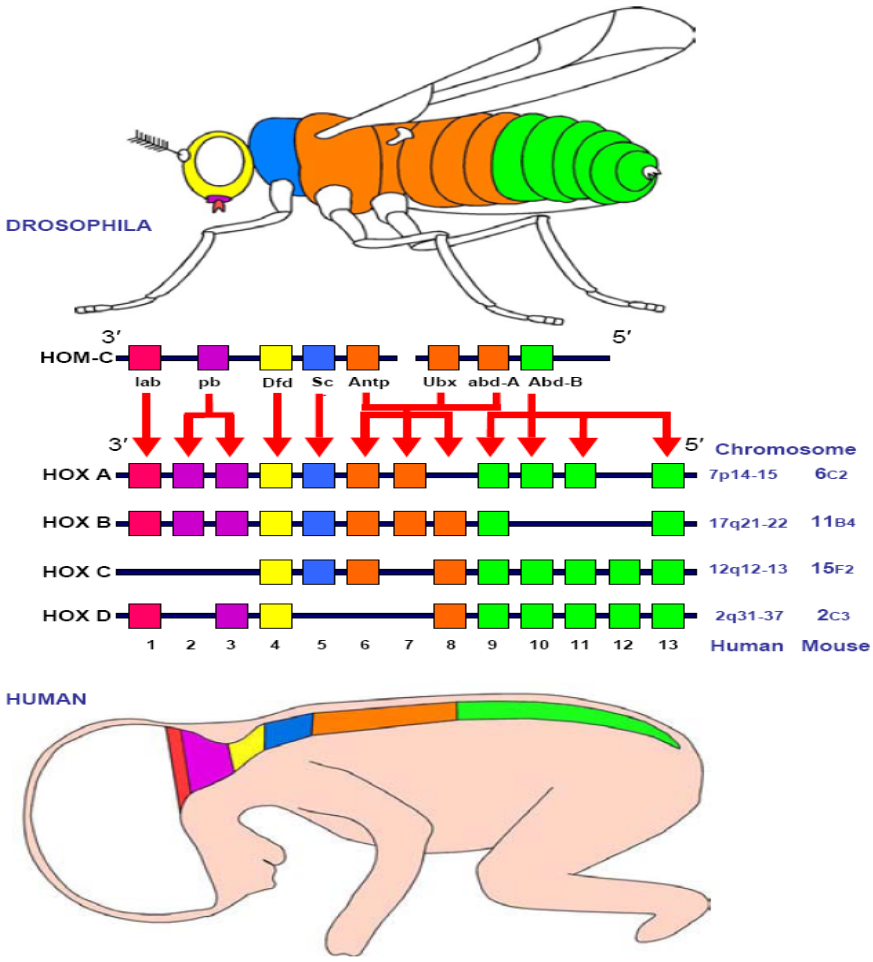

Figure 1: Conservation of collinear expression between HOM-C in drosophila and Hox gene clusters in mouse and human as cited in Lappin et al. The 3' genes are expressed earlier in the rostral region and the 5' genes are expressed in the caudal region of the embryo.

Hox genes are known to exhibit spatial and temporal co-linearity. The temporal expression pattern of genes within a cluster is spatially correlated with their position in the chromosome. For example Hox A cluster is in chromosome 6 and it has 13 genes, A1 to A13. Temporal co-linearity indicates that A1 (3' end of the cluster) will be expressed earlier during development than A2 and so on. Spatial colinearity can be defined as the correlation between the physical order of Hox genes in their chromosome cluster (from 3' to 5') and their domain expression along the AP axis: early expressed Hox proteins are found at the rostral part of the

embryo whereas later Hox expressed proteins are found at the caudal part of the embryo. Most important, this spatial and temporal co-linearity of Hox genes acts simultaneously in the all the cluster, trans-co linearity. This means that paralog Hox genes located in different chromosomes are co-regulated.

In overall, the co-linearity of Hox gene expression pattern inside the clusters and distribution of Hox proteins (Hox code) along the rostrocaudal axis of the embryo suggests that gene cluster organization is necessary to maintain Hox functional domains. Indeed, despite DNA sequence divergence between species, Hox genes cluster organization has been successfully retained during evolution. Rather than a universal mechanism, the temporal and spatial establishment of this co-linear pattern is regulated by a variety of, in principle, unrelated processes: cis regulatory sequences, global enhancer sequences that regulate gene cluster expression in a relatively promoter-unspecific manner and epigenetic marks that define chromatin domains that facilitate sequential transcriptional activation along the cluster (Tumpel et al, 2006, Kmita et al 2003). It is known that the cis regulatory sequences of orthologous clusters are conserved between species (Chiu et al, 2002) but they are not conserved between paralogous Hox clusters (Lehoczky et al, 2004). Relevant for this project, Hox gene activation is associated with nucleosome modification, chromatin decondensation, and chromatin looping out of the chromosome territory (i.e. higher order chromatin structural changes). Upon induction of Hox B gene expression by retinoic acid, the sequential activation of clustered genes paralleled (e.g, Hox B1) or preceded (e.g. Hox B9) the acquisition of histone modifications that mark active chromatin with subsequent chromatin decondensation (Chambeyron et al, 2004). However, any of this mechanisms can explain the phenomenon of trans-co-linearity or how Hox genes located in different chromosomes, paralogous genes, are co-regulated.

Our primary hypothesis is that nuclear architecture constitutes a higher order, evolutionarily conserved, regulatory mechanism that controls important aspects of Hox gene expression regulation. We believe that Hox genes nuclear orientation regulates the spatiotemporal co-linearity of the Hox gene in a cell/tissue specific manner beyond primary interactions of cis-regulatory sequences and upstream regulators. As the mouse embryonic cells undergo differentiation and become neural stem cells, there is an evident change in the shape of the nucleus. This may cause changes in nuclear orientation of the genes as the cells differentiate from embryonic stem cells to neural stem cells. Therefore, the null hypothesis for this project is that the position of Hox gene clusters in particular nuclear territories is determined by mechanical properties like displacement and force.

The packaging of the genome within different cell types is unique to the cell type as it allows cell type-specific gene expression and silencing patterns (Baylin et al, 2007). Since the cell encompasses a multidimensional organization of its components, the attempt to study the nuclear architecture also requires a multidimensional approach of analysis. Studies aiming at understanding the genome organization and functions of different elements of the nucleus should incorporate mathematical and engineering concepts that model the biological process. We used tridimensional (3D) fluorescence in situ hybridization (3D-FISH), 3D-reconstruction and quantitative image analysis to map the position of Hox gene paralogous clusters in individual nuclei. Together with mathematical modeling and statistical analysis we aim to establish an experimental platform to investigate the positional dynamics of Hox clusters during cell differentiation. This will provide a mechanical foundation for understanding the role that nuclear architecture plays in genome function.

Section 2: RESULTS AND DISCUSSION

2.1: Expression of Hox genes during embryonic stem cell differentiation toward the neural lineage.

Hox genes expression patterns were analyzed during mouse ESC differentiation to NSC. In order to achieve this, we performed a detailed characterization of both cell differentiation status markers and Hox mRNA expression at different time-points during the differentiation process.

Mouse ESC were transitioned to neural stem tissues (NST) and propagated to neural stem cells (NSC) according to protocols detailed in the Material and Methods section. This process requires roughly 15 days and it is illustrated in Figure 2. ESC grown in coated gelatin plates and in media supplemented with leukemia inhibitory factor (LIF) stayed in an undifferentiated stage forming characteristic colonies with well defined boundaries (Figure 2a). The initiation of the differentiation process starts upon re-plating the cells in serum-free basal media (N2B27) upon the withdrawal of LIF. Cell differentiation occurs in parallel to the colonies acquiring rosette morphology with cell protrusions (Figure 2b). Addition of FGF and EGF growth factors favors cell differentiation to the neural lineage by forming cell cluster floating aggregates known as neurospheres (Figure 2c) which are dissociated to single cells by tituration. These single cells adhere to the plate and become NSC cells with a characteristic bipolar morphology (Figure 2d) (see Material and Methods section for details).

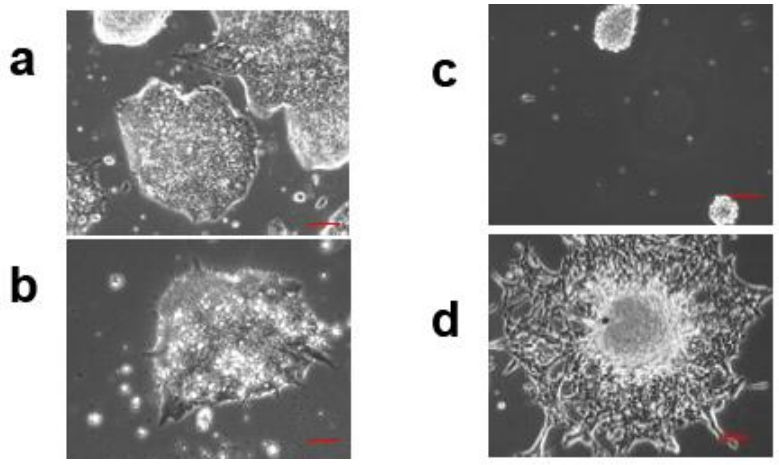

Figure 2: Differentiation of Mouse ES cells into Mouse NS cells. Scale bars are 100um

We sampled our cells at day 0 (ESC, Figure 2a), day 3 and 7 after the initiation of the differentiation process (Figure 2b), day 10 (neurospheres, Figure 2c) and day 15 (NSC, Figure 2d). The transition of ESC to NSC was confirmed by real time RT-PCR using specific markers, Nanog for undifferentiated ESC and Nestin for NSC. Our results show that ESC differentiation towards the neural lineage is correlated with the decreased expression of markers of cell pluripotentiality (Nanog) and with the increase of NSC markers (Nestin).

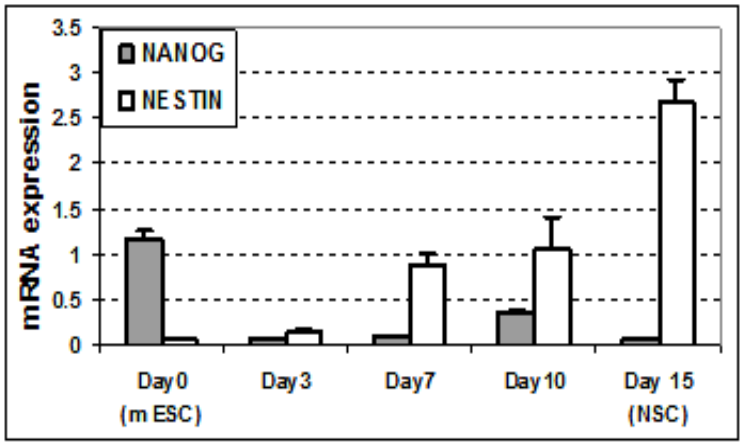

Figure 3: ***Hox gene expression on cell differentiation markers. Figure (left) indicate the Relative mRNA expression of the differentiation markers Nanog and Nestin, during the process of ESC differentiation towards NSC at the indicated time points. Each data point is the mean of values from 3 independent cell populations.***

On analyzing the expression of Hox genes at different time points of differentiation, it was found that there was a prominent expression of members of the four Hox clusters by day 7 (Figure 4). Hox gene activation at day 7 correlates with a remarkable increase of the neural marker Nestin (Figure 3) and with the first cytological indication of cell differentiation, a characteristic rosette morphology of the colonies (Figure 2b).Interestingly, we observe prevalence in the activation of Hox genes located in the 5' domain of the four cluster paralogs as cells commit to the neural lineage, exemplified by the upregulation of Hox B9, Hox C9, Hox D9 and Hox A13 mRNA expression, which is maintained in NSC. However, mRNA expression of 3' Hox cluster domain genes, including Hox B4 and Hox A4, are also upregulated at day 7 and 10, coinciding with the formation of cell cluster floating aggregates (neurospheres).

It was established in 1992 by Weiss and Reynolds that neural stem cells could be maintained by the propagation of floating cell cultures which they called ”neurospheres’ .These neurosphere cultures contain a heterogeneous cell population consisting predominantly committed progenitor cells combined with differentiated neural cells like astrocytes and neurons. This includes cells with stem cell-like characteristics as well as more restricted progenitor cells, which may explain mixed cell phenotypes and expression patterns. In NSC only the expression of members of the 5’ Hox domain was detected, correlating with previous reports showing that this domain is sensitive to FGF pathway regulation (Bel-Vialar et al., 2002). Moreover, these data support the model that the FGF signaling pathway may be involved in the preservation of the multipotent state of NSC by the establishment and/or maintenance of a progenitor Hox expression profile. Therefore, the regulation of the Hox expression patterns that occurs in parallel to FGF-induced differentiation of ESC toward the neural lineage is an excellent model to investigate the role of epigenetic gene regulation in the self-renewal and fate specification of stem cells during embryonic development.

This project is focused on the comparative analysis of nuclear positioning of the Hox genes within the two cell types: pluripotent embryonic stem cells (ESC) and neural (NSC) stem cells.

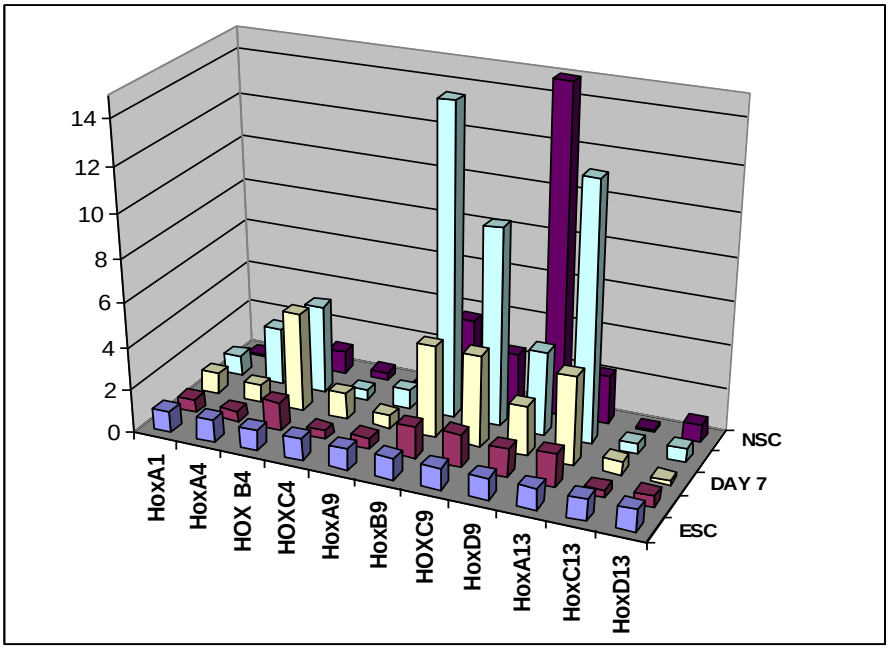

Figure 4: Real time PCR. Relative mRNA expression of Hox genes during the process of ESC differentiation towards NSC at the indicated time points. The data represent the fold induction of mRNA expression, over ESC levels, of the indicated Hox genes. Each data point is the mean of values from 3 independent cell populations. Error bars not shown (5-15% of the Mean in every sample, in left panel).

2.2: 3D nuclear organization of Hox gene cluster in ESC and NSC

Fluorescence *in situ* hybridization (FISH) was used in three-dimensionally preserved nuclei (3D-FISH) using Hox cluster specific probes. Each Hox cluster is represented by two overlapping BAC clones, giving approximately 500 kilobases of genome coverage. We use four different colors for simultaneous visualization of the four Hox clusters. DNA- DAPI counter stain is used to determine the nuclear volume. We only acquired cells in G1 phase before replication of Hox genes, which showed two distinct signals per cluster. 5 color-stained individual nuclei were acquired using a LSM510MTA confocal microscope (Zeiss, Thornwood, NY) (see Material and Methods for details).

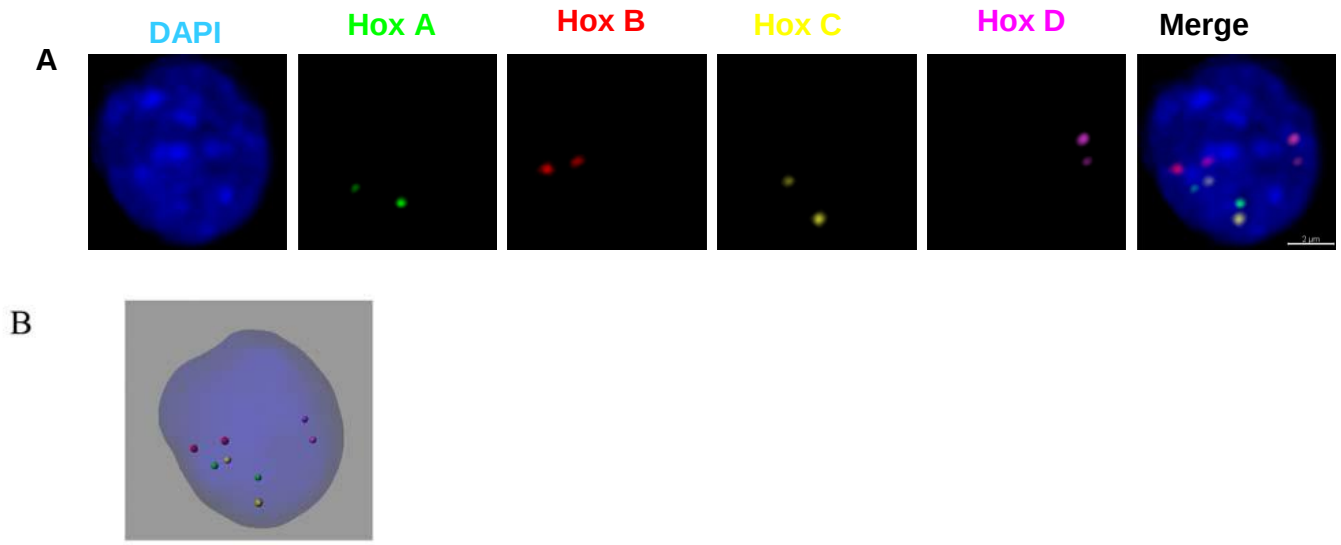

Figure 5: 3D-FISH of HOX genes in ESC. A) 2D projection of confocal image Z-stack. The 4 Hox clusters are represented by 4 different colors and the picture on the right indicate the combined effect seen with the DAPI staining. B) 3D reconstruction of confocal Z-stack images using Imaris Software.

Figure 5A shows the 2D projection of the confocal Image Z-stack. The nucleus is stained with DAPI and the 4 different Hox clusters are stained with different color markers. The figure 5B shows the 3D reconstructions of confocal Z-stacks. The quantitative image analysis was performed using Imaris software (Bitplane, A.G) (see Material and Methods for details). The software analyzes the images and gives accurate 3D Cartesian coordinates (x, y, and z) for each cluster. The nuclear volume, as defined by DAPI staining, is modeled as an ellipsoid. We recorded the distinct parameters of the ellipsoid: axes length and orientation and 3D coordinates of the ellipsoid center. These data are then used to calculate the distances between paralogous and heterologous clusters as well as to analyze the relative position of each Hox cluster loci in ESC and NSC nuclei for comparative statistical analysis. These analyses are shown in the sections below.

2.3 Nuclear Volume and shape on ESC and NSC.

As mentioned before, the nuclear volume was modeled as an ellipsoid in both cell types. This normalization brings different cell nuclei to a common shape platform, which facilitates comparative analysis of nuclear architecture between ESC and NSC. We first calculated the volume and sphericity index for each individual nucleus of both cell types. Sphericity can be defined as a property of an object when it approaches the geometrical shape of a sphere, which is a tridimensional symmetrical entity.

Our results show that the nuclear volume as well as the sphericity index is different between both cell types. We find that there is a general trend in the decrease of volume as well as sphericity in NSC. However even though the nuclear volume changes significantly (p-value is 0.012 for alpha value 0.05), the most remarkable differences between cell types is related to their sphericity index (p-value - 6.6 E-05) (Figure 7). Indeed, NSC is elongated and flat as compared to ESC as seen in figure (6).

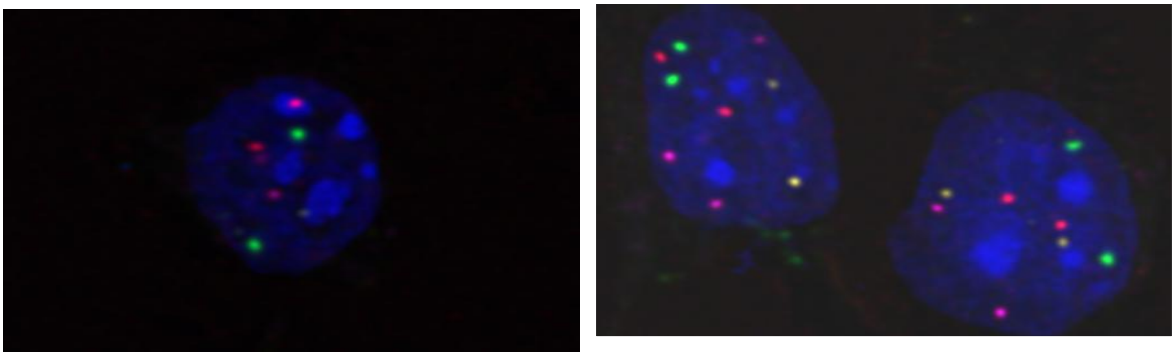

Figure 6: DAPI staining of individual nuclei of ESC (left panel) and NSC (right panel).

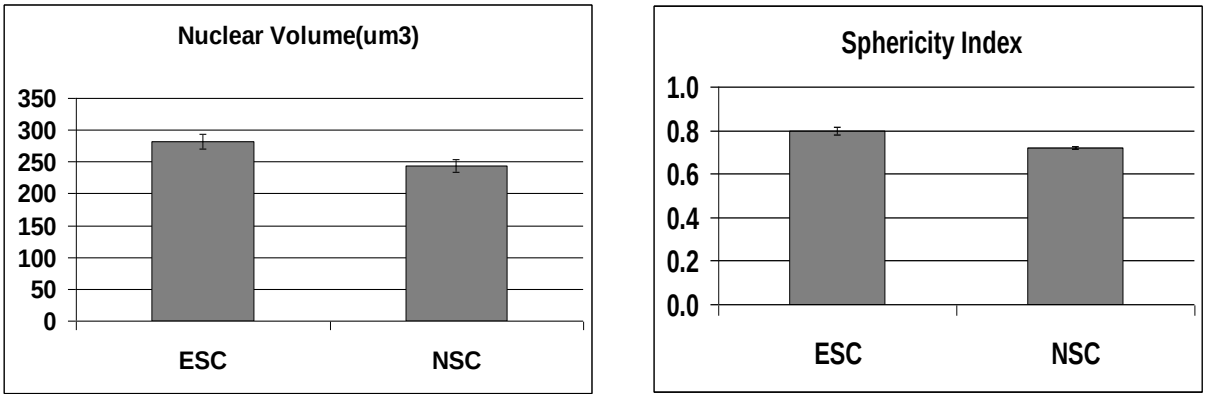

Figure 7: Mean values of the nuclear volume (um3) (left panel) and sphericity index (right panel) for ESC (n=32) and NSC (n=42). P- Value for volume between the two cell types is 0.012 indicating significant change in nuclear volume between cell types. P- Value for sphericity between the two cell types is 6.6E-05 indicating a very significant change in the shape of nucleus as the cells differentiate to the neural lineage.

To further analyze the differences observed in the change of nuclear shape between ESC and NSC we compare the aspect ratio of both cell types, which is another parameter associated with the ellipsoid axis. This parameter is calculated as the ratio of the semi-minor axis to the semi-major axis. Our software models the cells as an ellipsoid and gives the values for all the three axes for each and every cell .The quotients obtained by dividing the value of semi-minor axis by its corresponding semi-major axis for each cell is calculated. We take the mean of all the quotients for 32 ESC and 42 NSC. The results are shown in figure 8. It is evident that the NSC gets elongated along the semi-major axis and reduced along the semi-minor axis when compared to ESC.

These observations provides the base for our null hypothesis which postulates that changes in nuclear shape, as the cells differentiate to the neural lineage, determine the reorganization of Hox clusters position in NSC as compared with ESC nuclei.

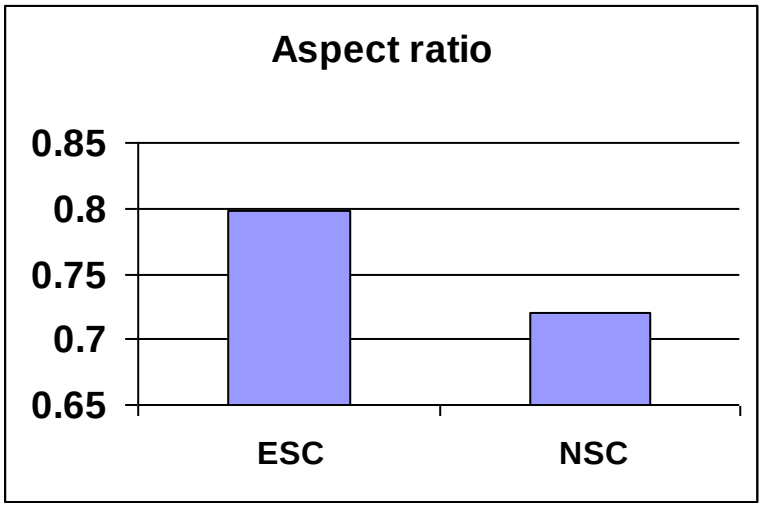

***Figure 8: Aspect ratio of the mean of the 32 ESC and 42 NSC. As seen from the figure above the aspect ratio of the ellipsoid for ESC and NSC indicate the elongation of the semi-major axis for NSC*.**

2.4: Distances between Hox cluster.

Walter Fitch in 1970 (Systematic Zoology 19:99-113) defined paralogous genes to be homologous genes resulting from gene duplication so that both copies have descend side by side during the history of an organism. Paralogous indicates “para” which means “in parallel”. HOX genes are highly conserved evolutionarily genes believed to be originated in protozoans by duplication and divergence from one ancestor homeobox gene. Mammals have 38 Hox genes housed on four clusters (A to D) located on 4 distinct chromosomes and each cluster conforms up to 13 Hox genes. For example, Hox A cluster in chromosome 7 and has 13 genes, A1to A13.The co-linearity of Hox gene expression pattern inside the clusters contributes to the anterior posterior embryonic patterning. These 4 Hox clusters located in different chromosomes are the paralogous Hox clusters. Each Hox gene in mammals contains two exons and one intron. The homeobox is located on second exon in Hox genes and exhibit a homology between paralog groups. The distances between these four clusters with one another are called “Distance between the heterologous gene clusters”. In addition, as mammals are diploid organisms there are two copies of each chromosome which are homologous chromosomes.

The distance between Hox clusters located in the homologous chromosome pair is called "Distances between the Homologous gene clusters".

We calculated the distances between both heterologous and homologous Hox gene clusters by using the 3D Cartesian coordinates provided by IMARIS software. This analysis was done for 32 ESC and 42 NSC individual nuclei.

Let the given coordinates for one cluster A be x_1, y_1, z_1 and the coordinates for cluster B be x_2, y_2, z_2 , the distance between cluster A and B is calculated by the formula: $\left[\sqrt{x_2-x_1\ ^2+\ y_2-y_1\ ^2+\ z_2-z_1\ ^2}\right]$.

Normalization between cells was achieved by taking the ratio of the distance between the individual Hox clusters in a given nucleus by the respective cell's nuclear volume.

2.4 (a): Distances between homologous clusters:

Interallelic distances between homologous Hox clusters were calculated using the 3D coordinates as indicated above. The results of the mean of the distances are shown in Figure 9 and the percentage frequency distribution is shown in Figure 10. ANOVA comparative analysis of mean values was only significant for the Hox A cluster (P-value- 0.003), although we see a general tendency of cluster interallelic distances to increase in NSC as compared with ESC. (See colocalization of Hox cluster for further discussion).

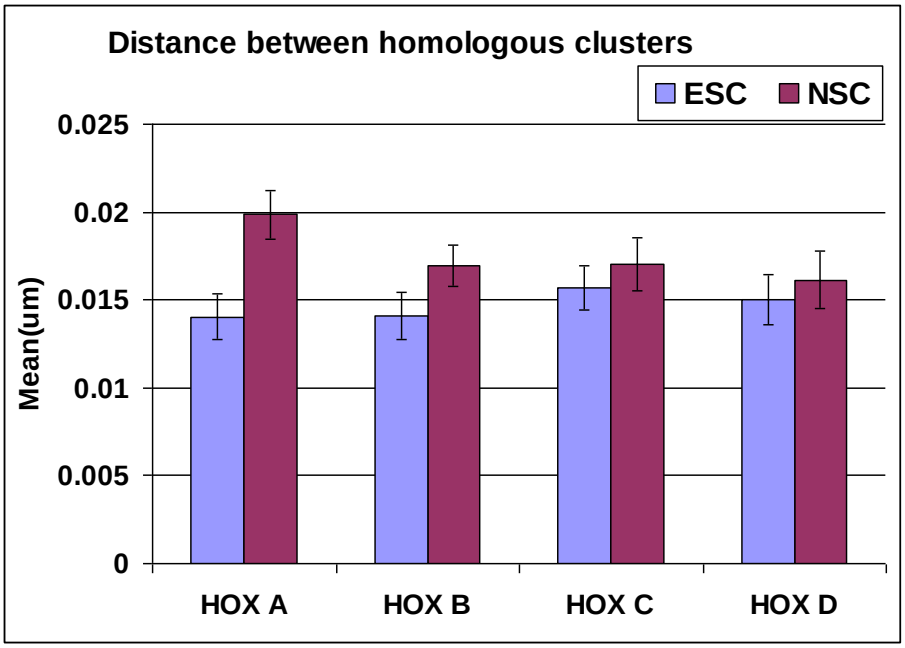

Figure 9: Mean of the interallelic distance between the homologous pair. ESC (n=32) and NSC (n=42).No significant differences in mean values was observed for Hox B, C and D. Mean of the interallelic distance between the homologous pair normalized by individual cell volume. ESC (n=32) and NSC (n=42).No significant differences in mean values was observed for Hox B, C and D. For Hox A the p-value was 0.003 indicating a significant shift in Hox A clusters in NSC.

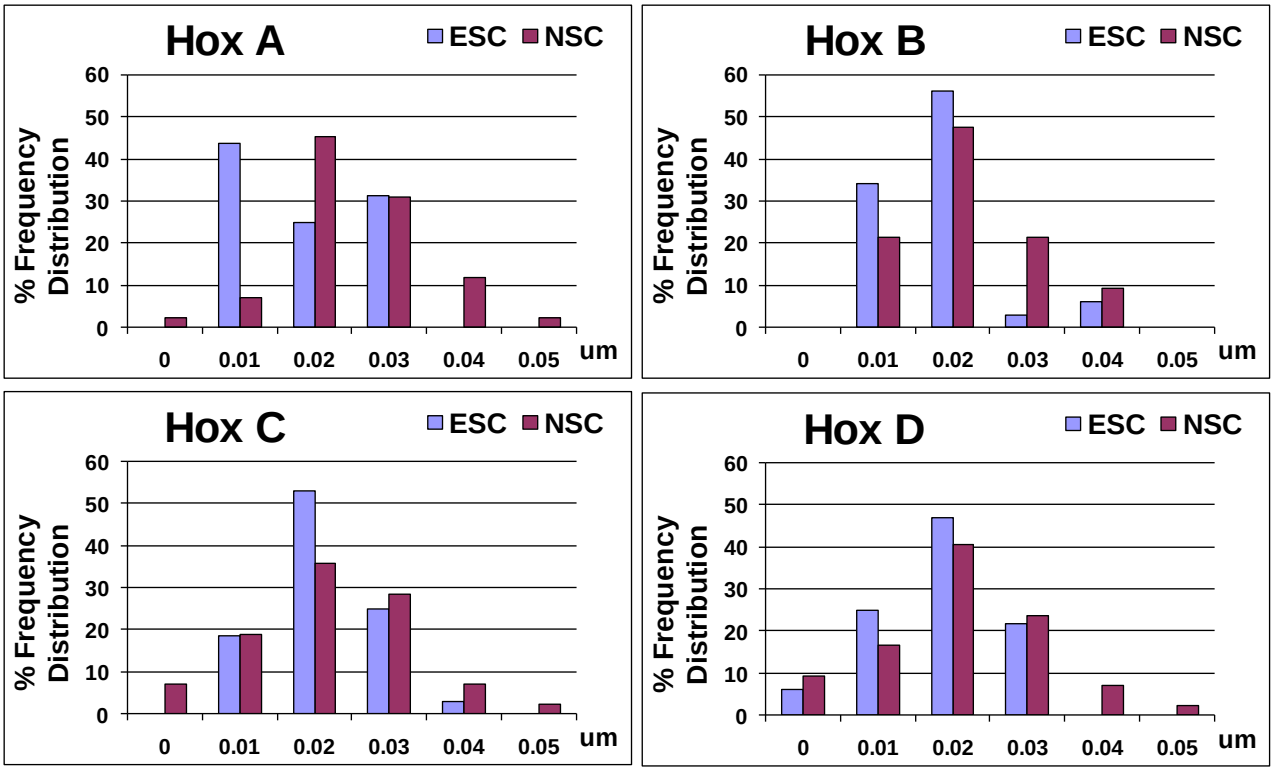

***Figure10: Histograms of the frequency distribution of the interallelic distance between the paralogous pair in ESC and NSC for each cell normalized by volume*.**

2.4 (b): Distance between heterologous clusters:

The distances between heterologous clusters were calculated using the 3D coordinates as indicated above. The results of the mean of the distances are shown in Figure 10 and the percentage frequency distribution is shown in Figure 11. Since we have two alleles for each gene, we get 8 Hox cluster foci per nucleus. Using permutation-combination we get 128 values for ESC (32 cells) and 178 values for NSC (42 cells) of heterologous pairs distances.

Distances between heterologous clusters increase significantly in NSC as compared with ESC (Figure 10 and 11). ANOVA statistical analysis (alpha 0.05) was used to compare the mean values of the distances between heterologous clusters: Hox A-B (P-value - 0.0005), Hox A-C (P-value- 1.27E-06), Hox A-D(P-value- 0.003), Hox B-C(P-value- 0.0003), Hox B-D (P-value -0.0003) and for Hox C-D(P- value- 0.01). These results indicate that clusters located on different chromosomes do actually move away from one another as the cells get deformed and differentiated. However, even though the distance between heterologous clusters increases in NSC as compare with ESC, the interallelic distance between the Hox clusters for Hox B, C and D does not change between cell types. Therefore, even though the changes in the heterologous clusters are significant it is still difficult to conclude that nuclear shape actually contributes to the movement of Hox clusters away from each other in NSC as compared with ESC. There may be other factors that contribute to the relative movement of these clusters related with their proper transcriptional regulation. It has to be however noted that the small sample size may have contributed to slight variations in data.

Most of the previous work on Hox clusters and their nuclear arrangement have been based on only one parameter “distances”. Since the nucleus is a 3D entity, this measurement is insufficient to draw and conclusive answers as it can give stochastic outcomes. Moreover we

might need a huge sample size and large data collection involving very cumbersome techniques.

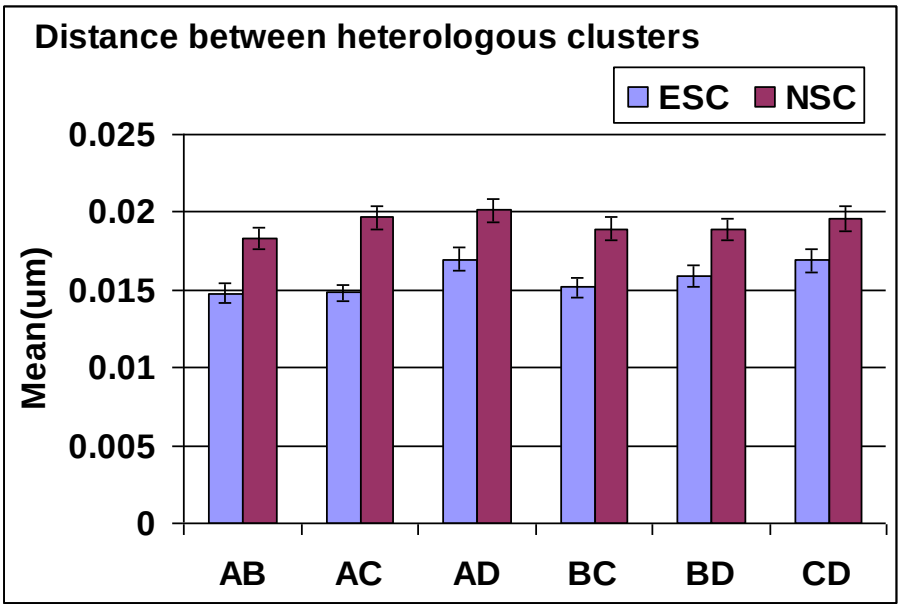

Figure 10: Mean of the distance between the heterologous pairs of the clusters in the nucleus of ESC and NSC normalized by volume.

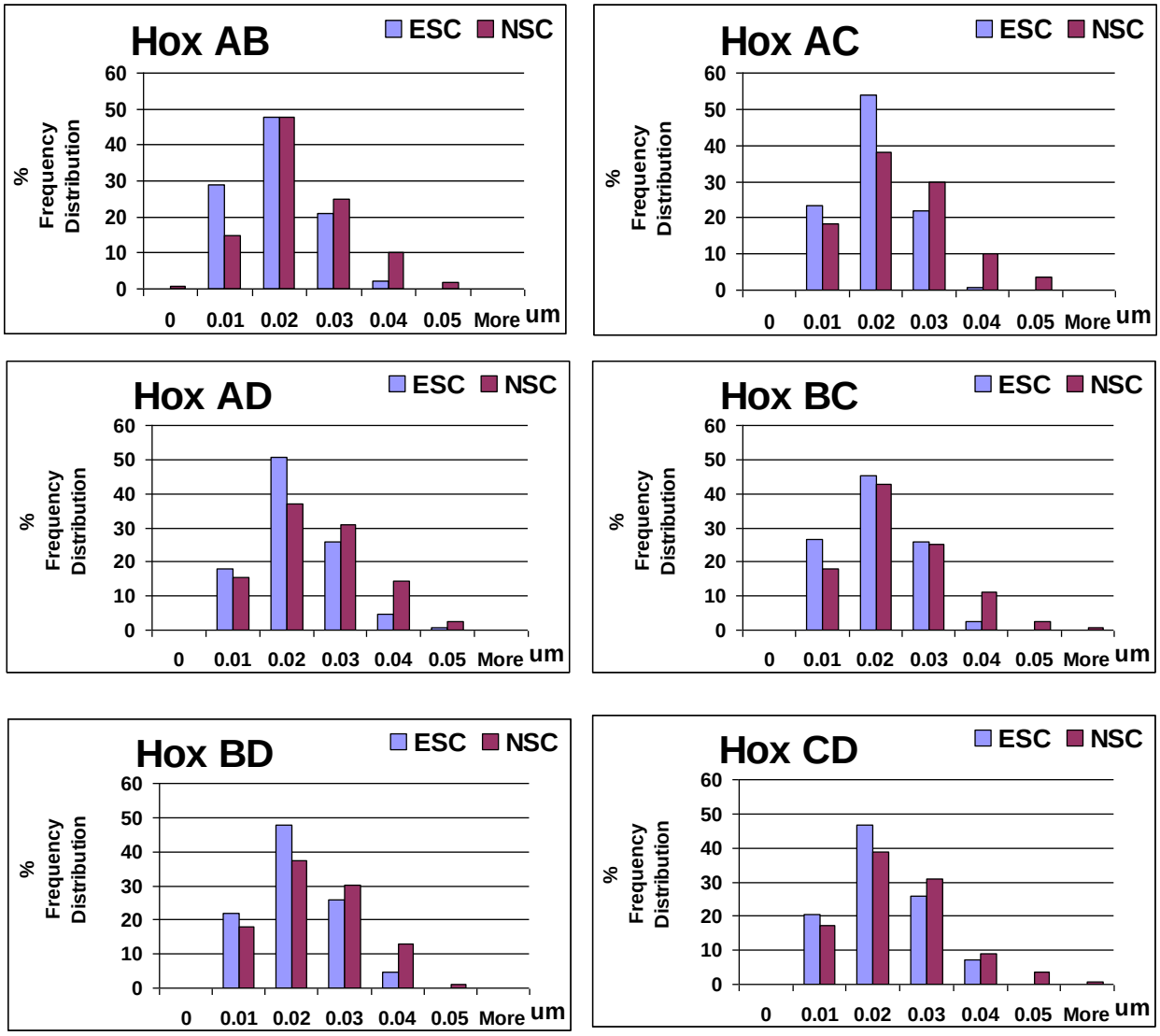

Figure 11: Histograms of frequency distribution of heterologous clusters taken with 32 ESC and 42NSC for each cell normalized by volume. There is a relative increase in the distance between different Hox clusters in NSC.

2.4 (c): Colocalization of Hox clusters:

As we discussed in the Introduction Section, a particular phenotype may involve the clustering of genes and regulatory sequences located in different chromosomes. Prominent examples include the regulation of the globin genes (α and β globin genes) (Brown et al., 2006), olfactory receptors (Lomvardas et al., 2006) and regulation of X chromosome inactivation in

females (Xu et al., 2006). Brown et al studied the correlation of α- and β-globin genes at successive stages of terminal erythroid differentiation. The α- and β-globin genes lie on different chromosomes and have different chromatin contexts. The study shows that the α- and β-globin are away from one another when silent, but are located in close proximity at splicing factor enriched nuclear speckles when transcriptionally active. However they do not colocalize. Lomvardes et al similarly study the nuclear organization of olfactory receptor genes correlated to its transcriptional regulation. The authors studied how the association of the H enhancer element which lies on chromosome 14 with different olfactory receptor (OR) gene promoters which are located on different chromosomes. The H enhancer element functions in cis on its adjacent OR cluster or in trans on OR promoters which are located on different chromosomes. In other cases, long range interactions between genes located in different chromosomes is related with genomic imprinting. Gene imprinting can be defined as the differential gene allele's expression in a parent-of-origin-specific manner. An imprinted gene expresses only the allele inherited from the mother or from the father or one of the alleles is randomly inactivated. The common example of gene imprinting is X chromosome inactivation in mammals. Females inherit two X chromosomes. Males inherit one X chromosome and one Y chromosome. In order to equalize the expression of X linked genes between males and females, one X chromosome is inactivated in females. This is called X chromosome inactivation (XCI) and it is controlled by specialized DNA sequences that conform the X-inactivation centre (*Xic*). The physical association or close proximity of the two X chromosomes is necessary to achieve X chromosome inactivation (Bacher, 2006; Xu, 2006). Bacher et al, 2006 specifically suggested that before any X chromosome inactivation, the two *Xic*s transiently colocalize. Despite the examples mentioned above and the growing literature on the nonrandom positioning of the genes and chromosomes and their relative effect on the specific patterns in the nucleus (review from Mistelli et al,2004),the relative functional relevance of long-range gene interactions in the overall genome regulation and the DNA regulatory elements that govern it is still not known.

The colocalization or overlapping of genes located on different chromosomes is known as “kissing’’ of the genes (Lanctot et al., 2007). We proposed that the physical organization of the interphase nucleus coordinates the expression of Hox paralog genes situated on different chromosomes. This can be achieved by favoring long-range chromatin motions that facilitate direct contact between heterologous Hox clusters. In this case, we expect that Hox paralogs (heterologous) cluster spacing will decrease at the time when they are simultaneously activated. This will indicate that the proximity of Hox gene regulatory sites, such as cis elements and epigenetic modifier binding elements, is necessary for the coordinated expression between paralog Hox gene clusters.

In figure 12 we show the frequency distribution of the distances between combined homologous and heterologous (paralogs) clusters of the 32 ESC and 42 NSC nuclei: We get 128 homologous pairs in ESC and 168 homologous pairs in NSC; 768 heterologous combinations for ESC and 1008 for NSC. There is a significant change in the distances between the homologous (p-values for ANOVA is 0.005) as well as heterologous (p-values for ANOVA is 2.4E-16) clusters when we combine distances between all the clusters. Despite the small sample size, we observed nearly 8% “kissing events” in NSC between homologous alleles. However, only 1 “kissing events” (0.7%) was observed between the homologous alleles in ESC. We do not see any “kissing events” among the heterologous clusters even though the total number of heterologous combinations is larger as compared to homologous pairs.

Our results indicate that homologous Hox genes physically associate in NSC and not in ESC. This may be related with genomic imprinting transcriptional regulation, which is more relevant in NSC where Hox genes are expressed.

We did not observe any “kissing events” in heterologous clusters indicating no physical association between these clusters. As mentioned before, we expected that the distance between paralogs (heterologous) spacing would decrease at the time when they are simultaneously activated as consequence of its transcriptional co- regulation. Our results suggest that the collinear regulation between the Hox gene cluster is not a simple phenomenon of physical contact between gene clusters in agreement with previous reports (Lanctot , 2007). Though the main drawback of the previous mentioned report are mixed cell population and a small sample size. In this project we made a bold effort to avoid mix cell populations as it is indicated by our results of robust Hox gene expression profiles in both ESC and NSC (see section 1 for expression analysis). However even our sample size may be not sufficient to detect any sporadic events. It has been suggested that large macromolecule machineries that regulate chromatin structure and function are formed by stochastic interactions of single subunits (Misteli, 2001a). This dynamic system favors the idea that relatively low-abundance proteins, roaming the nucleus looking for binding sites, frequently encounter specific target sites (Misteli, 2001a). Considering that many genes are only regulated sporadically and that most replication and repair sites only require the presence of a few copies of a particular component, probabilistic interactions of factors with chromatin are sufficient to sustain their functionality. This can be translated to gene regulatory interactions. Indeed, it is known that long range chromatin motions in addition to being of functional relevance are very rare events that occur as a result of specific physiological responses (Chuang, 2006). According with this data, a larger sample size will increase the probability of observing the physical association of the heterologous clusters. Additionally, most of the research till date focuses on the gene localization based on the distances from nuclear center or nuclear periphery or between different gene loci. As the cells are polydimensional entities, calculations and analysis based on distances alone is an over simplification of the system which does not cover all the parameters involved in a 3D nucleus. Hence the analysis based on only distances does not give us a comprehensive overview of the

gene positioning in the cells. A mathematical model considering all the other parameters, such as Hox cluster orientation and locational preference with respect to other entities within the nucleus will be a better approach to understand the multidimensionality of the Hox gene positioning in the cells. This gives a better probabilistic map of each Hox cluster in a 3D nucleus.

Moreover, the physical association of heterologous clusters may be regulated by some other specific factors, as the simultaneous association of cluster with functional nuclear components. Indeed, the nuclear position of a gene locus and its association with specific nuclear domains, such as the nuclear periphery and the nucleolus, is correlated with its activity, and that this occurs in a cell type and cell differentiation status specific manner (for a review see (Ruault, 2008)). According with these facts, we propose to use immunohistochemistry in parallel to FISH analysis to identify other fiduciary markers within the nucleus including components of the nuclear envelope and nucleolus. These landmarks can be used to aid the analysis of 3D map of Hox gene clusters and to identify specific nuclear elements of functional relevance that that correlate with transcriptional activation or repression of Hox genes.

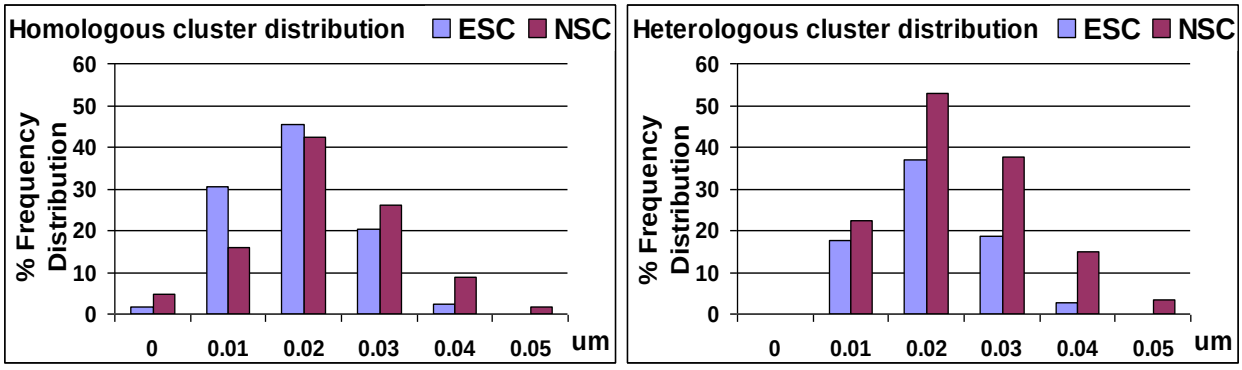

Figure 12: (left panel) and (right panel) indicates the percentage frequency distribution of Homologous clusters and heterologous clusters respectively .The data are taken by normalizing the distances within each cell by its respective volume.

2.5 Angular distribution of Homologous Hox clusters with semi-major axis:

We know that as the cells get differentiate, there is a change in the shape of the cell nucleus. We hypothesize that as the nucleus gets elongated in NSC, a parallel change in the distances between the homologous clusters will occur. Each individual homologous cluster's distance, which is a vector, will form a particular angle with the semi-major axis of the nuclear ellipsoid. As the nuclear shape changes we expect that the orientation of this vector with respect the nuclear axes to change accordingly. For example, if the elongation of NSC when compared with ESC is due to a decreased length of the semi-major axis then the distance between homologous clusters that lie in parallel (0 degrees) to semi-major axis should decrease proportionally. On the contrary, if there is an elongation along the semi-major axis where the length of semi major axis increases and then the distance between the homologous pair that lie parallel to the semi major axis also increases. On the other hand, if the elongation in NSC is caused due to the increase in semi-minor axis then the distance between homologous clusters that lie in perpendicular (90 degrees) to the semi-major axis should increase. If there is a decrease in the length of the semi-minor axis then the distance between the homologous pair which lies perpendicular to the semi-major axis should decrease proportionally.

We use this analysis to test our null hypothesis which postulates that as cells undergo differentiation there is a change in the reorganization of Hox clusters position in the nucleus to accommodate the nuclear shape change (elongation) in NSC. In summary, we checked our null hypothesis by analyzing the correlation between the magnitudes (distance) of the homologous cluster, which is a vector, with the angular distribution that this vector forms with the semi major axis of the ellipsoid (nucleus). This gives us two vectors. One vector formed by the distance between homologous clusters and the second vector formed by the semi-major axis of the nuclear ellipsoid. The magnitude (distance) of the vector is defined by the 3D coordinates of the

end point of the vector. We calculated the angles between the vectors formed by the homologous cluster and the semi-major axis vectors using the cosine rule as in the following example:

We assume the coordinates of the homologous cluster A to be ax_1, ay_1, az_1 and ax_2, ay_2, az_2 . The coordinates at both ends of the semi-major axis are given by px_3, py_3, pz_3 and px_4, py_4, pz_4 . We calculate the difference in the distances between the x, y and z coordinates for each vectors involved and assign them as a, b, c for cluster A and a_1, b_1, c_1 for semi-major axis. This gives

$$a = ax_2 - ax_1$$
$$b = ay_2 - ay_1$$
$$c = az_2 - az_1$$
$$a_1 = px_4 - px_3$$
$$b_1 = py_4 - py_3$$
$$c_1 = pz_4 - pz_3$$

Now we calculate the angle (theta θ) between the two vectors by the formula

$$\cos\theta = a \times a_1 + b \times b_1 + c \times c_1 \div \left[\sqrt{a^2 + b^2 + c^2}\right] \times \left[\sqrt{a_1^2 + b_1^2 + c_1^2}\right]$$

Figure14 shows the frequency distribution of the angles formed between the homologous cluster vectors with the semi-major axis for both ESC and NSC. The distribution of angles in ESC is very similar for all the clusters (p values > 0.1), which are evenly spread from 15 to 75 degrees. As shown in Figures 8 and 9, we do not observe a significant change of the distances between specific homologous pair for Hox B, C and D clusters in ESC and NSC. However for Hox A there is an exception. Therefore, there is no a general correlation between the angle formed by the vectors in ESC and the displacement of interallelic distances between cell types.

However, the distribution of angles in NSC is not similar between clusters (p- values for Hox C and Hox D were 0.02). Moreover, when you compare the angle distribution between cell types, there are statistical significant differences for cluster A, B and D (p values- 0.008, 0.004, 4.33 E-05, respectively). These results indicate that homologous chromosomes change their alignment with respect to semi-major nuclear axes but there is no significant change in the interallelic distances between cell types. These results suggest that Hox gene interallelic distances are conserved between cell types. However, as the cells differentiate and change the nuclear shape, the chromosomes containing the Hox paralogs gets re-oriented in a different angle with respect the nuclear major axis in order to be accommodated for the change in shape of the cell nucleus. In other words, the nuclear deformation makes the vector formed by the homologous chromosomes to re-orientate itself inside the cell nucleus instead to changing its magnitude.

In overall our results suggest that nuclear volume and shape are not dictating the nuclear positions of Hox genes cluster and that there are other forces that orient them to their targeted positions. So our null hypothesis does not hold true.

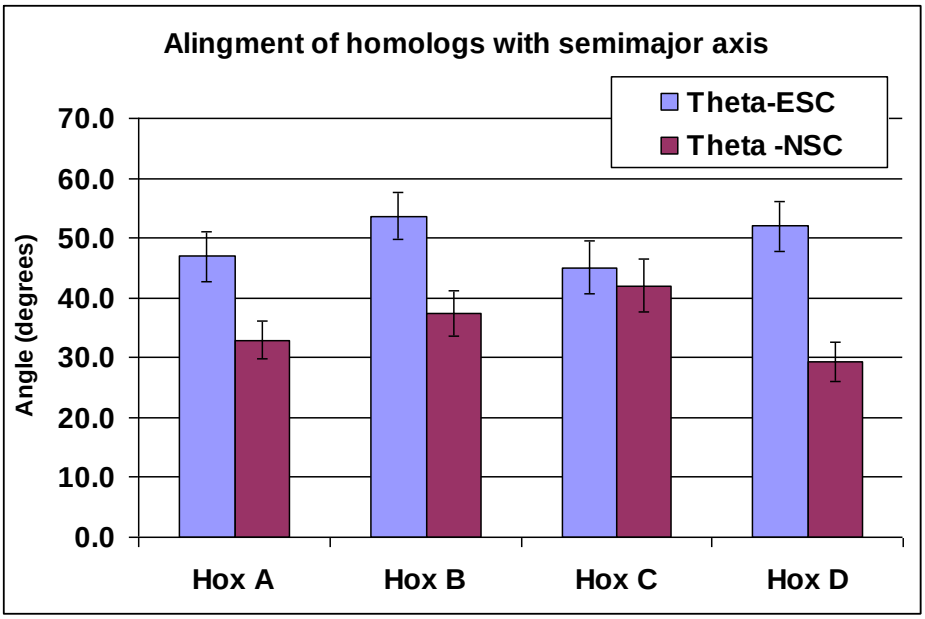

Figure 13: The mean of the angles the paralogous cluster create with the semi-major axis.

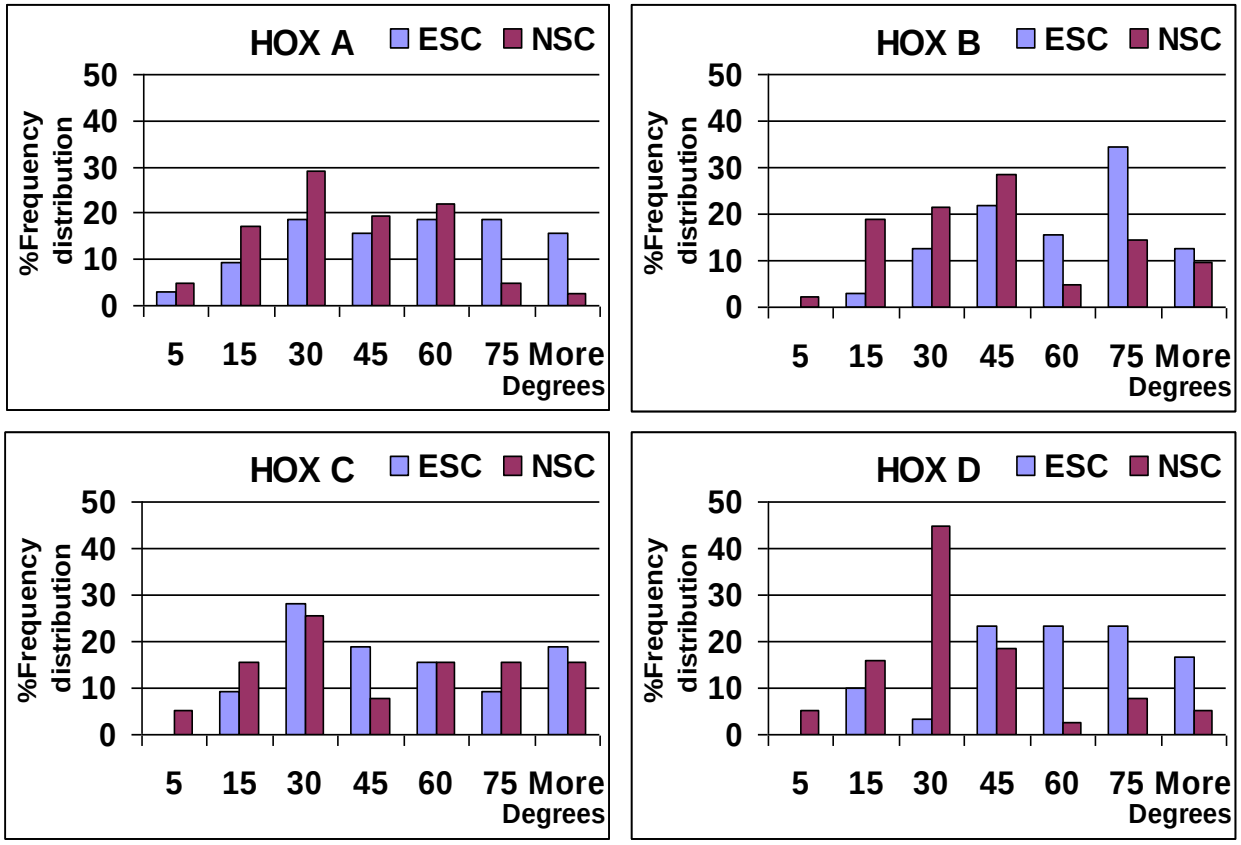

Figure 14: Histograms of the frequency distribution of Hox clusters with respect to the semi-major axis of the ellipsoid.

2.6 Radial distribution of the Hox cluster position

The chromosome positioning with respect to the nuclear center and periphery can be summed up under radial distribution. Radial distribution of gene and chromosome territories in 3D acquired nuclei has been previously investigated using a model developed by Cremer et al in 2001 (Cremer and Cremer, 2001a). The authors use a voxel (volume element)-based algorithm base in the intensity distribution of DAPI-stained DNA. The nuclei were modeled by a "shell" methodology where the nuclear space was divided into 25 equidistant shells with a thickness of $\partial r = 1 \div 25 \; r_0$ where $r_0 = 100$ is the distance between nuclear center and any point on the segmented nuclear border. Thus modeling the nucleus as a sphere of radius r_0=100. This was used for all the cells independently of their respective shape and volume. The distance from each voxel to nuclear center (r) was calculated as a fraction of r_o for each voxel located in the nuclear interior. All the voxels for a given CT were identified and florescence intensities were summed up for 100% for each shell for normalization in every cell. Cremer defined average radial distribution as the average relative DNA content in nuclear shells as a function of the relative distance *r* from the 3D center .The same principle was used in Hepperger et al. 2008 (Hepperger et al, 2008).

We did a comparative analysis of radial distribution of Hox genes in both the cell types using a more accurate analysis by using a precise mathematical model as compared with previous reports (Cremer et al, 2001). Our model is based in absolute positions (3D Cartesian coordinates) of each and every voxel of the image. Therefore, the concept of "shell" methodology is avoided as we can calculate the specific distances that connect our clusters which we get as 3D Cartesian coordinates. Moreover, we modeled the nucleus as its natural ellipsoid shape instead to reshape it as a sphere, which it is a more accurate model considering

the shape of the NSC. For each nucleus we calculated the volume based on DAPI staining and also the specific parameters of the ellipsoid including the center coordinates and axes length.

The line equation defined by connecting the center of the ellipsoid (nuclear center) and a particular locus (Hox cluster) point, will also intersect the nuclear periphery (ellipsoid surface) at a unique point “p”. Thus, the coordinates of the “p” are shared by both the ellipsoid and the line equations. Given the center of the ellipsoid coordinates, “p” can be calculated by resolving ellipsoid and line equations. To calculate the coordinates of the point “p”, we first translate each and every Hox cluster coordinate to the center of the nucleus by assigning the nuclear center as $x = 0, y = 0, z = 0$. Translation can be defined in Euclidean geometry as moving every point in a specified direction to the origin by making the origin (0, 0, 0), facilitating subsequent calculations. For example, we have a cluster A with coordinates x_1, y_1, z_1 on a line joining center (0,0,0) and the point p x_2, y_2, z_2 .Now this gives us a simple and easy way to calculate the point on the ellipsoid which also intersects with the line that the cluster A joins with the center of the nucleus (0,0,0).

The generalized equation for any point with 3D coordinates x, y, z on the ellipsoid is given by $x^2 \div a^2 + y^2 \div b^2 + z^2 \div c^2 = 1$ where x, y, z are the coordinates of any point on ellipsoid and a, b, c are the semi-major, semi-minor and z axis of the ellipsoid respectively. This gives us a parametric equation for ellipsoid passing through Hox cluster A to be

$$x_1^2 \div a + y_1^2 \div b + z_1^2 \div c = 1 \text{------} Equation(1)$$

Where x_1, y_1, z_1 are the coordinates of Hox cluster A in the ellipsoid and a, b, c are the semi-major, semi-minor and z axis of the ellipsoid respectively.

This also gives us a parametric equation for ellipsoid on the point P to be

$$x_2{}^2 \div a + y_2{}^2 \div b + z_2{}^2 \div c = 1 - - - - - - Equation(2)$$

Now the line passing through Hox cluster A (x_1, y_1, z_1) and center (000) will have a parametric equation that gives us the following equations below with an unknown variable "t'.

$$x_2 = 0 + x_1 - 0 \times t = x_1 t - - - - - - Equation(3)$$

$$y_2 = 0 + y_1 - 0 \times t = y_1 t - - - - - - Equation(4)$$

$$z_2 = 0 + z_1 - 0 \times t_1 = z_1 t - - - - - - Equation(5)$$

Substituting equations (3), (4) and (5) in equation (1) we solve for the unknown variable 't' .To find the point on the ellipsoid through which this line passes we will take into account the point that lies on the positive or first quadrant. It is important to know that the line will actually pass touch the ellipsoid at two points as it passes through the center on either sides. We substitute the coordinates of the line into the equation of the ellipsoid and solve for t

$$x_1 \times t \div a^2 + y_1 \times t \div b^2 + z_1 \times t \div c^2 = 1 - - - - - - Equation(6)$$

Equation (6) gives us a value of "t" as we know the values for $x_1, y_1, z_1, a, b,$ and c. Substituting the value of "t" from equation (6) in equation (2), (3) and (4) we calculate the coordinates for P x_2, y_2, z_2 .

This allowed us to calculate the exact distances from the center of the nucleus to the "p" point (radius, "r") and to the locus (Hox cluster, "d"). The radial distribution of a particular locus is defined by the ratio d/r, where 0<d/r<1 (where 0 denotes the center of the nucleus and 1 represents the nuclear envelope or periphery).

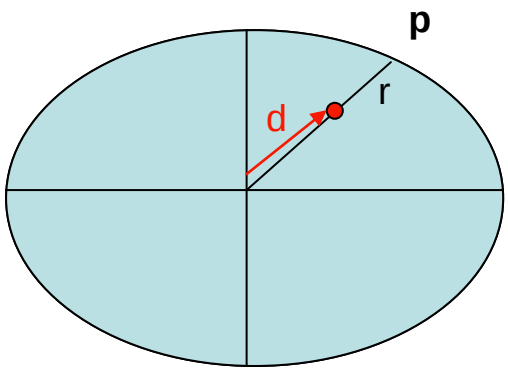

***Figure15: Indicates the shape of the ellipsoid as the cells are modeled. 'd' indicates the distance of the Hox clusters from the center of the nucleus and 'r' indicates the distance of the point that lies on the line joining the clusters to the center as well as the point that lies on the periphery from the center*.**

The mean and the frequency distribution of the radial parameters for all Hox cluster are shown in figures 16 and 17. The results indicate that there is no significant change in the radial distribution of Hox A, B and C gene clusters between ESC and NSC. However, there is a significant shift for the Hox D cluster with a (P- value of 0.003) towards the nuclear center in NSC as compared with ESC. We can conclude from the angular distribution as well as the radial distribution that there is a change in the orientation of Hox D cluster in NSC as compared to ESC. This is despite the fact that there is no significant change in the interallelic distances between the homologous pairs of Hox D.

As we mentioned before, CT radial distribution changes during the cell cycle. It is also known believed to be influenced by chromosome gene density (gene rich and gene poor chromosomes) and by the size of the chromosome. Gene rich- CT are located towards the center of the nucleus versus gene-poor CT close to the nuclear envelope or periphery (Cremer , 2006b; Cremer , 2006b; Cremer and Cremer, 2001b; Bickmore , 2004; Meaburn , 2007). This rule also applies to specific sub-chromosomal domains. It is known that gene dense domains in chromosomes are preferentially located towards the nuclear interior as compared with gene

poor domains (Neusser et al 2007). It is known that Hox B and C are known to be located in gene rich chromosomes and accordingly, Hox B cluster is reported to be located towards the interior of the nucleus. Hox D gene is gene rich but is of large size. Previous reports shown that Hox D is preferentially located towards the nuclear periphery (Lanctot , 2007). However, our results show that Hox D in NSC moves toward the nuclear interior in parallel with its transcriptional activation. There are reports suggesting that Certain Hox gene loci ,during active transcription tend to be positioned on the chromosome surface forming loops (S.Chambeyron et al., Genes Dev.,p1119(2004)).With all these above mentioned data we can state that gene expression regulation depends on local DNA sequences ,epigenetic modification, higher order chromatin condensation and nuclear organization.

We use the location of the positioning of Hox clusters in two cell types as a genetic tool to analyze the relationship between the shape of the nucleus and the orientation of the Hox clusters between the two cell types. This also gives us and overall idea in deciphering the role of nuclear architecture in the regulation of Hox genes as it is an important in the characterization of diseases which are associated due to the chromosome rearrangements beyond DNA coding sequences. All these finding have contributed to analyze the orientation of the Hox genes clusters to some extend but we are still unable to conclude in our observation if any there exists is any correlation between the radial distribution of Hox cluster and either the gene content or the size of the host chromosome.

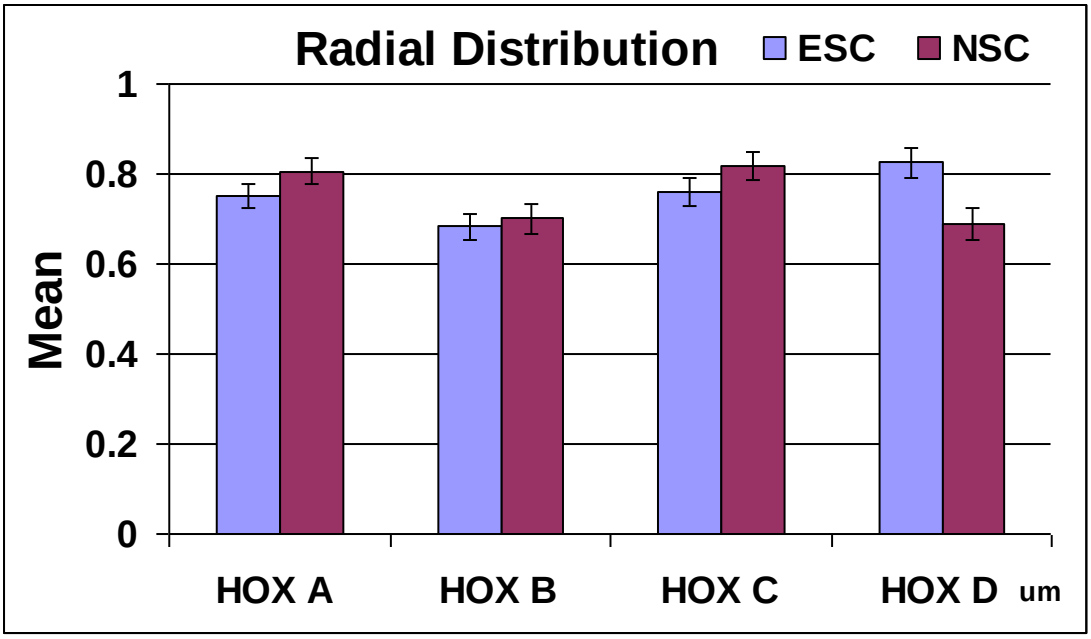

Figure 16: Mean of the radial distribution of Hox clusters in 32 ESC and in 42NSC Only Hox D is significant (P-value for Hox D- 0.003).

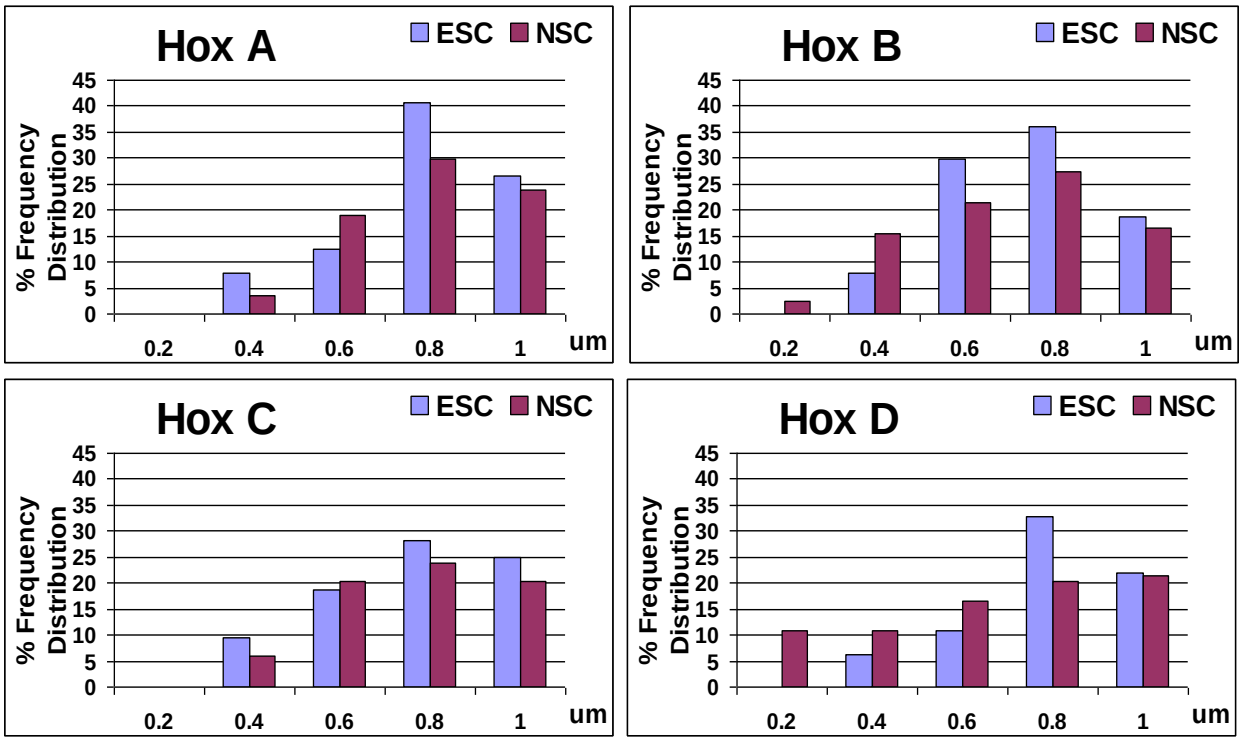

Figure 17: Histograms of the frequency distribution of Hox clusters for Radial distribution.

Section 3: Mathematical Model of 3D nuclear architecture.

Our main aim is to analyze the role of nuclear shape and architecture in regulation of Hox gene positioning in the nucleus and their expression. We know as cells differentiate there is a change in the shape of the nucleus justifying our null hypothesis which states that as the changes in nuclear shape happens as the cells differentiate to the neural lineage there is a possibility of the reorganization of Hox clusters position in NSC as compared with ESC nuclei in order to accommodate the change in shape.

However simple analysis of Hox clusters orientation based on distances alone does not provide a comprehensive coverage of all the dimensions of a 3D nucleus. Hence we use the concept of mathematical modeling where even a small data and give a precise overview of the intricate functioning of the Hox cluster orientation in the nucleus. We model the DAPI stained nuclei to be an ellipsoid and the individual Hox gene cluster positioning as 3D coordinates. Using these parameters we try to identify the change in relative locational positioning of Hox gene cluster in both the cell types. By focusing on a multidimensional modeling which includes distances between the homologous clusters, paralogous clusters, angular distribution of clusters and radial positioning of these clusters we try to analyze the relative positioning and features of the Hox clusters in both the cell types.

Our approach is similar to previous reports (Bergen et al., 2009), which is based on the 3D modeling with DAPI stained nuclear volume and by modeling the nucleus as an ellipsoid. We do get precise 3D Cartesian coordinates for each and every Hox cluster in the nucleus. We model the system by bringing the nucleus of all the cells to a common spatial platform. We used the concept of affine transformation on each and every Hox cluster in the cell nucleus. Affine transformation consists of linear transformation along with translation, rotation and

inversion. The use of affine transformation helps us create a normalized platform for the comparison between nuclei of both cell types to analyze the positional mapping of the Hox gene clusters. The position of the new transformed coordinates for the clusters can be calculated using the following methods.

Translation: This is the first step and it involves the uniform movement of all the points in one particular direction. In our case this is achieved by reassigning the nuclear center as (0, 0, 0) and recalculating Hox cluster nuclear position accordingly. This is done by subtracting the nuclear center coordinates of each nucleus from each and every 3D coordinates of all the Hox clusters loci within that nucleus. This makes all the center of all nuclei to have a common nuclear center (0, 0, and 0) as a common point of reference.

Rotation: The second step is to rotate each of the three nuclear ellipsoid axes to a common axis orientation. The software uses a common plane of reference (picture frame) to calculate the coordinates of every pixel of the image. Therefore, the Hox cluster coordinates of a given nucleus are calculated with respect to this plane of reference independently of the orientation of the nucleus inside the picture frame. In order to compare different images, we need to bring the nuclear axis (ellipsoid axis) of all the cells to align together. Now we do an axis rotation to orient the ellipsoid axis in nucleus in such a way that all the ellipsoid axis of each and every nucleus (images) will lie in the same orientation. We do this by rotating the new translated coordinates of each cluster with respect to the ellipsoid with common orientation. This is achieved by calculating the matrix “a”, which is a matrix for the rotation of all the three axes of each ellipsoid modeled nuclei (semi-major axis, semi-minor axis and the Z- axis) in all the three directions (X, Y, Z) giving us a 3 rows and 3 column matrix with a total of 9 components. Let that matrix be defined by ‘a’ with the components as shown in equation (7).

$$\text{a} = \begin{pmatrix} a_{11} & a_{12} & a_{13} \\ a_{21} & a_{22} & a_{23} \\ a_{31} & a_{32} & a_{33} \end{pmatrix} ------Equation(7)$$

The calculation for each component in the matrix is as follows:

For the semi-major axes components are calculated as shown in equation 8, 9 and 10. Let a, b, c are the semi-major, semi-minor and z axes of the ellipsoid. Let ax, ay, az be the unit vectors of the a-(semi-major) axis for each cell.

$$a_{11} = \left[a \times ax + b \times ay + c \times az \right] \times ax \div \sqrt{a^2 + b^2 + c^2} ------Equation(8)$$

$$a_{12} = \left[a \times ax + b \times ay + c \times az \right] \times ay \div \sqrt{a^2 + b^2 + c^2} ------Equation(9)$$

$$a_{13} = \left[a \times ax + b \times ay + c \times az \right] \times az \div \sqrt{a^2 + b^2 + c^2} ------Equation(10)$$

Similarly for the semi-minor axes components are calculated as shown in equation 11, 12 and 13. Since a, b, c have be defined as the semi-major, semi-minor and z axes of the ellipsoid, we assign bx, by and bz to be the unit vectors of semi-minor axis b-(semi-minor) axis for each cell.

$$a_{21} = \left[a \times bx + b \times by + c \times bz \right] \times bx \div \sqrt{a^2 + b^2 + c^2} ------Equation(11)$$

$$a_{22} = \left[a \times bx + b \times by + c \times bz \right] \times by \div \sqrt{a^2 + b^2 + c^2} ------Equation(12)$$

$$a_{23} = \left[a \times bx + b \times by + c \times bz \right] \times bz \div \sqrt{a^2 + b^2 + c^2} ------Equation(13)$$

Finally for the Z-axis components the calculations as shown in equation 14, 15 and 16. As mentioned above a, b, c have be defined as the semi-major, semi-minor and z axes of the ellipsoid .Here we assign cx, cy and cz_z to be the unit vectors of Z axis.

$$a_{31} = \left[a \times cx + b \times cy + c \times cz \right] \times cx \div \sqrt{a^2 + b^2 + c^2} ------Equation(14)$$

$$a_{32} = \left[a \times cx + b \times cy + c \times cz \right] \times cy \div \sqrt{a^2 + b^2 + c^2} ------Equation(15)$$

$$a_{33} = \left[a \times cx + b \times cy + c \times cz \right] \times cz \div \sqrt{a^2 + b^2 + c^2} \quad ------Equation(16)$$

For example one of the cluster A in the cells is modeled as a point by Imaris with Cartesian coordinate (x,y,z).The translation of the coordinate to the center (0,0,0) gives new coordinates $A_1(x_1, y_1, z_1)$. After rotation for normalization it will move to $A_1'(x_1', y_1', z_1')$ position by using the formula

$$A_1' = a \times A_1'$$

The new coordinates of Cluster A will be

$$x_1' = x_1 \times a_{11} + y_1 \times a_{12} + z_1 \times a_{13}$$

$$y_1' = x_1 \times a_{21} + y_1 \times a_{22} + z_1 \times a_{23}$$

$$z_1' = x_1 \times a_{31} + y_1 \times a_{32} + z_1 \times a_{33}$$

This gives us the new rotated coordinates for the cluster Hox A .This is the end result of translation and rotation.

Inversion: Cells are oval in shape and all of them will have DAPI stained nucleus and 4 distinctive Hox Cluster markers. When the images of the cells retrieved from the microscope are analyzed to identify the top and bottom of each cell, it has been concluded that these markers are insufficient to analyze the orientation of the Hox clusters in the cell.

By using Inversion methodology these drawbacks of images taken during cell positioning of the slide can be eliminated and provide a uniform platform to analyze all the cells. Every cell will have eight Hox clusters and these clusters will be located either above or below the semi-major axis. In order to have a uniform orientation of all the clusters with one point of reference we randomly select Hox B cluster as that point of reference and assume that by applying the

inversion technique we will have the majority of Hox B clusters above the semi-major axis. This could provide sufficient data for the analysis.

The basis for applying the inversion technique is by multiplying the Y-coordinates of all the Hox clusters with (-1) in the cells where either one or both the Hox B clusters (point of reference) are located below the semi-major axis.

Graphs:

We use Matlab to create scatter plot of the distribution of Hox gene clusters in ESC as well as NSC. The scatter plots after the affine transformation are shown in figure 18 and 19. These plots indicate the distribution for Hox A, Hox B, Hox C and Hox D for both the cell types in a common platform. In ESC each cluster seems to be occupying non-overlapping individual nuclear domains. On the contrary, heterologous clusters tend to occupy a common nuclear domain in NSC. Hox B tends to be more scattered in NSC but are especially closer towards the nuclear center in ESC. Hox D seems to be preferentially positioned towards the nuclear center in NSC as compared to ESC.

In order to make the analysis easy, the graphs shown in Figures 18 and 19 can be into four quadrants. By observing the quadrants of the two figures it can be observed that Hox C is not present in the fourth quadrant for ESC as well as for NSC. The scatter plots after the final affine transformation indicate that the Hox genes are prominently distributed towards the center in ESC and are positioned along the vertical direction in a top-down manner. However this is not seen in NSC where the Hox genes are more scattered in the horizontal direction and are relatively less randomly distributed in terms of a top-down manner. The homologous Hox gene clusters in ESC inspite of being densely packed towards the center do not overlap where as in NSC they do overlap even though they are scattered.

However even with a small sample size our mathematical model gives a comprehensive view of the Hox cluster orientation in the nucleus for comparision between the ESC and the NSC. Modeling gives a better approach rather than considering only the distances which gives only one parameter. Our chances of large “kissing events” would have been possible with a large number of data as these colocolization are rather schotactic. We would anticipate more colocolization in NSC if we had a larger sample size.

One of the drawbacks of this project was the lack of additional fiduciary markers that aids to orient the nucleus in a defined direction. In a very recent report, a statistical map of gene territories in live yeast has been performed using a similar approach of what we use in this project (Berger, 2008). The authors also used 3D coordinates of the fluorescent specific locus and the nuclear center. Individual cell nucleus was also modeled as an ellipsoid. In addition, they also segmented the nucleolus as a nuclear landmark, helping them to reorganize the nucleus of all the cells to a common orientation. For future work we will use additional fiduciary nuclear landmarks to improve the mapping of the gene clusters. This will help us attain another dimension to the axis rotation (Z –axis) of the ellipsoid. It helps in simplifying the layout of the gene locations with respect to two entities: the nuclear center as well as the nuclear marker making the calculations and the modeling more precise and accurate.

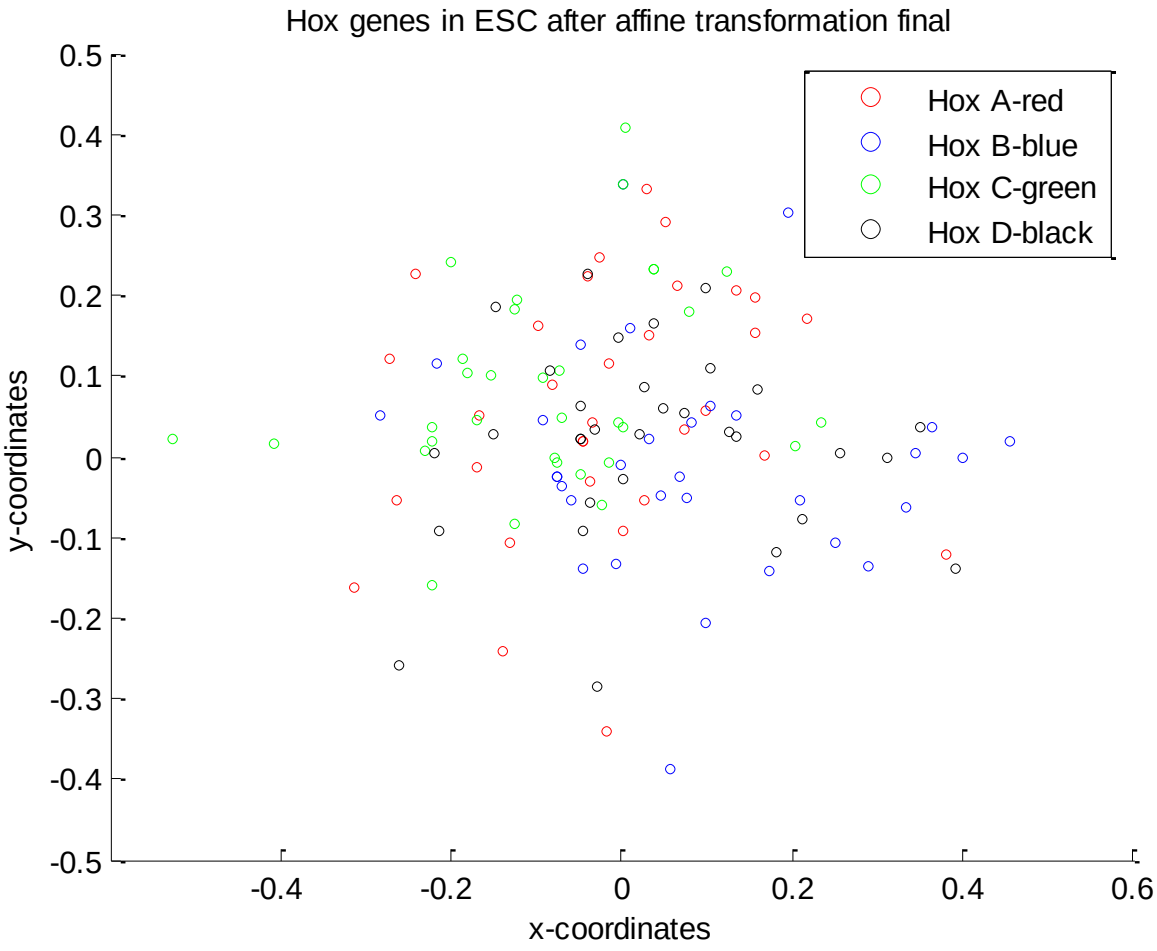

Figure 18: Scatter plot for ESC after affine transformation

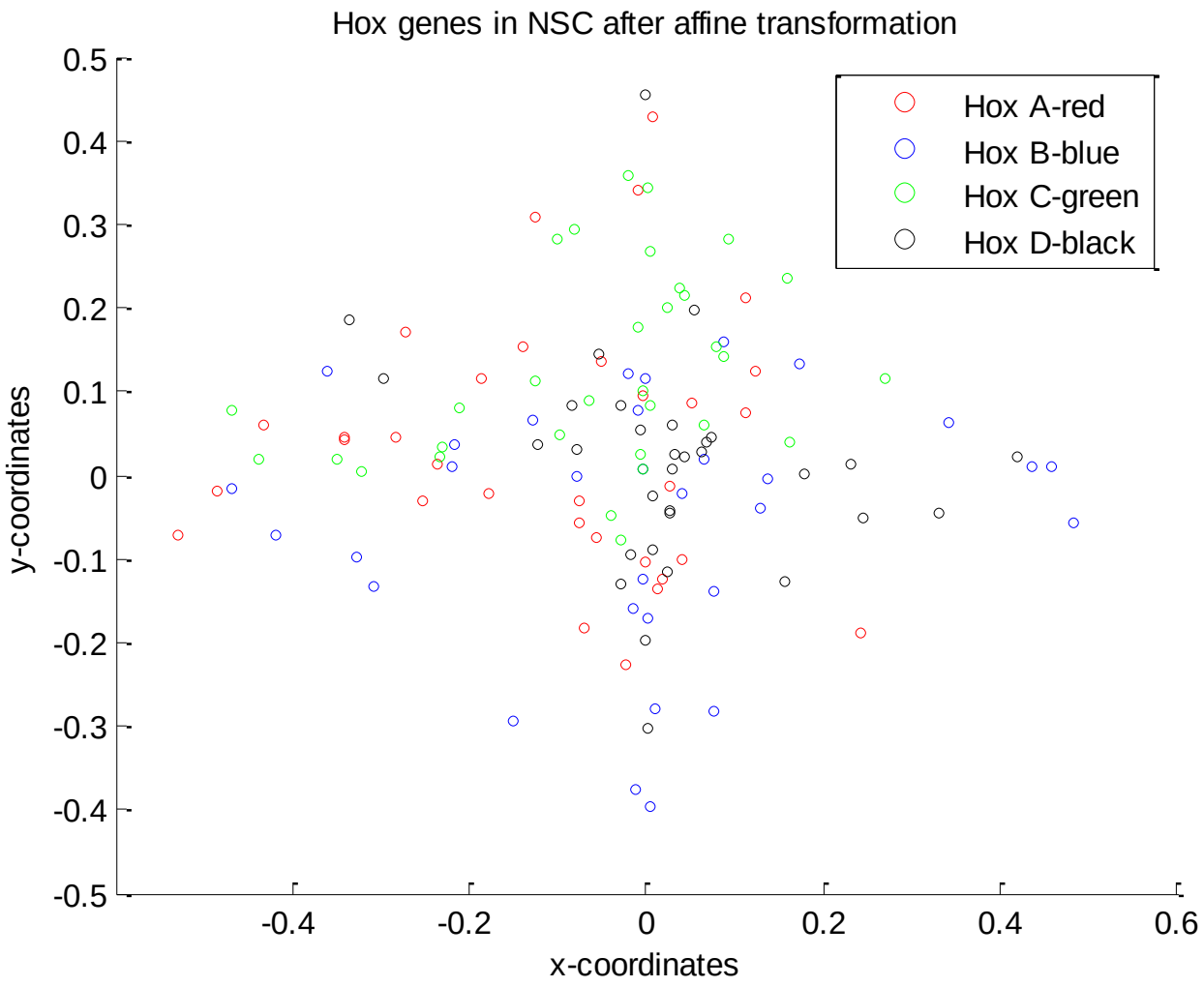

Figure 19: Scatter plot for NSC after affine transformation.

Section 4: Material and Methods:

Transitioning of ESC to NSC: mESCs transition toward NSCs was performed as described (Conti , 2005). Briefly, mESC were propagated in DMEM media with L-glutamine, supplemented with 10% of both fetal bovine and new born calf serum, 24.3 uL B-mercaptoethanol (Sigma) and 10ng/mL LIF (Chemicon International) on 0.1% gelatin plates. To transition ESC to NST, cells were propagated in 0.1% gelatin plates in N2B27 media (99 mL DMEM/F12, 96 mL Neurobasal Media, 1 mL N2 (1:100), 1 mL B27 (1:50) and 1 mL L-glutamine). The media was changed every 2 days. To obtain NSC aggregates, 10ng/ml of both FGF and EGF growth factors were added daily to the NST culture without change media for 3 days. Cell cluster floating aggregates (neurosphears) were harvested and titurated (12X) to dissociate to single cells. Cells were plated on uncoated tissue culture dishes in NS-A media (200ml of Neurobasal Media, 2 mL N2 (1:100) and 2 mL Penicillin/Streptomycin) supplemented with 10ng/ml of both FGF and EGF daily. Soon thereafter, the aggregates adhered to the plate and become NSC cells with a characteristic bipolar morphology.

RNA Isolation and quantitative RT-PCR: Total RNA from cultured cells was purified using RNeasy kit (Qiagen, Valencia, CA) and reverse transcribed using the Taqman Reverse Transcription Reagent kit (Applied Biosystems). Real time RT-PCR were performed using SYBR Green MMX (ABI Systems) on a GeneAmp 7900HT Sequence Detection System (Applied Biosystems), following the product manual protocols. All analyses were carried out in triplicates. Standard curves of serial dilutions of a control cDNA were used to determine the mRNA levels in individual samples. Expression levels were calculated as a ratio of the mRNA level for a given gene relative to the mRNA level for glyceraldehyde-3-phosphate dehydrogenase (GAPDH) in the same cDNA.

Primer design for RT-PCR: The primers were designed to target Hox paralog genes representative for each of the four Hox. These include Hox paralog group 4, 9 and 13 clusters. All these primers were design to expand exon-Intron boundaries to avoid genomic DNA amplification. The primers used are given below:

HoxA1F; GATGAAAGTTAAAAGAAACCCTCCC;

Hox A1R; CCACGTAGCCGTACTCTCCAAC;

Hox A4F; AAGAAGATCCACGTGAGCGC;

Hox A4R; GCTTAGGTTCGCCTCCGTT;

Hox A9F; ATCGATCCCAATAACCCGG;

Hox A9R; CTTCTTCCGAGTGGAGCGAG;

Hox B4F; GCAGGTCCTGGAGTTGGAGA;

Hox B4R; CGCGTCAGGTAGCGATTGTAG;

Hox B9F; TACGCTTCTGGCAAACAGTCC;

Hox B9R; TGCGATGTTTGCCTCTTTCC;

Hox C9F; TCTGCTTTTGGCTGCACATG;

Hox C9R; CATATCTCATCAGGGACCCCC;

Hox D4F; ACAGGTATCTGACCAGGCGC;

Hox D4R; GACACAGGGTGTGAGCGATTT;

Hox D9F; GCTGCTCGCTGAAGGAGG;

Hox D9R; ATTTGGTGTAGGGACAGCGCT;

HoxA13F; TCCCCACCTCTGGAAGTCC;

HoxA13R; TCTGAGGGATGAGAGACCACGT;

Hox B13F; CATTCTGGAAAGCAGCGTTTG;

Hox B13R; ACAGCCGTCGGGAGGAG;

HoxC13F; TCTGGAAGTCCCCCTTCCC;

Hox C13R; TGCTCACCTCGGGCTGTAG;

Hox D13F; GTACTGTGCCAAGGATCAGCC;

Hox D13R; GTAGACGCACATGTCCGGC;

NESTIN F; AGGCTTCTCTTGGCTTTCCTG;

NESTIN R ; TCCCAAGGAAATGCAGCTTC;

BAC clones: We selected BAC clones which expand Hox cluster genomic sequence. Appropriate BACS were obtained from CHORI. We selected two BACS per Hox. Their locations are given in the following charts:

For Hox A on chromosome 6

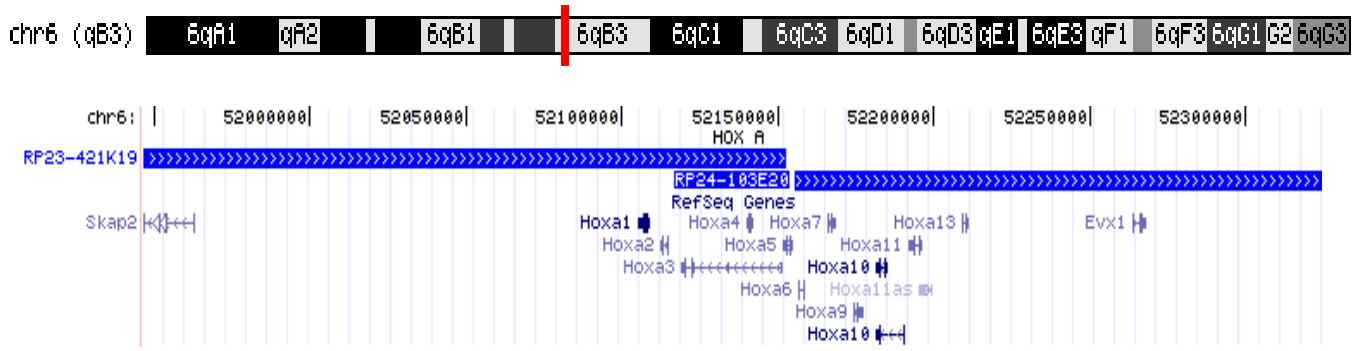

For Hox B on chromosome 11

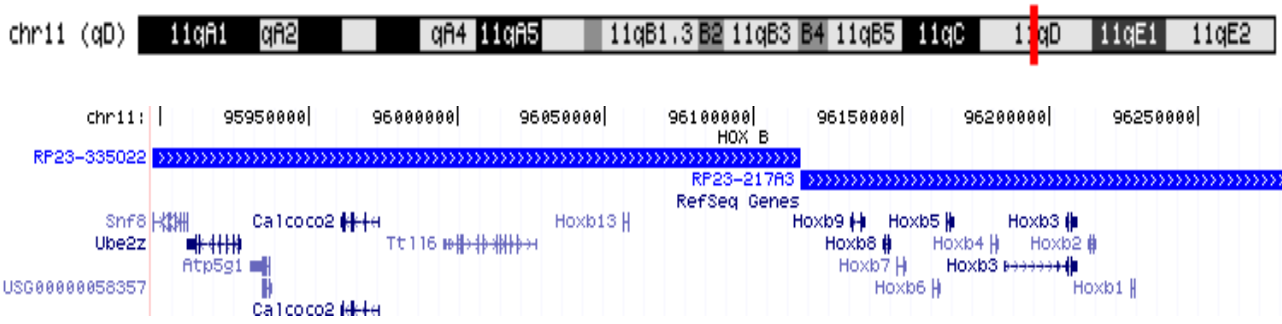

For Hox C on chromosome 15

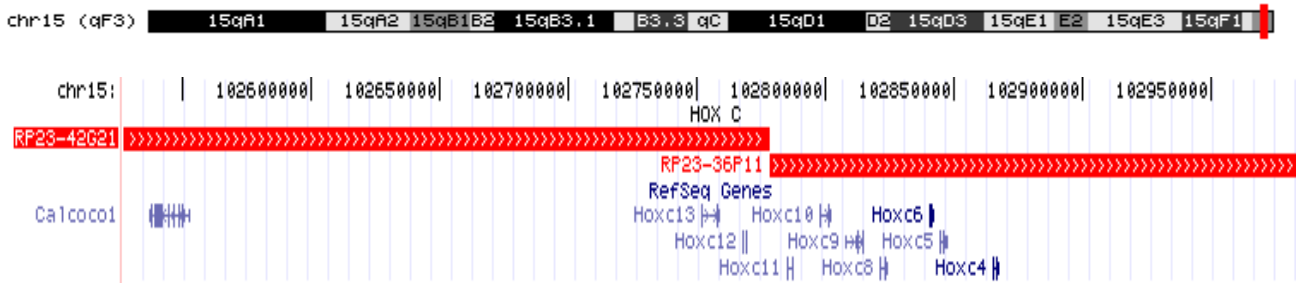

For Hox D on chromosome 2

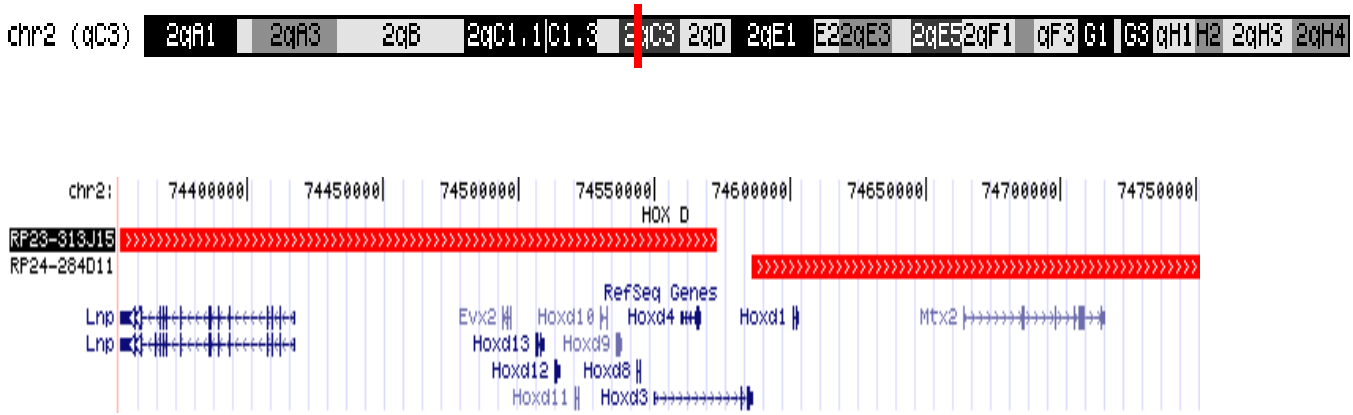

Each figure above depicts the red line on the chromosome where the insertion of the BAC clone begins. One clone covers 3' to 5' and the other in an opposite direction covering the whole clusters of the respective Hox clusters.

FISH: Fluorescence in situ hybridization is a unique technique that allows the detection and localization of a specific DNA sequence on a cell nucleus or chromosome. Our protocol involves the following steps: Nick translation, Ares reaction, slide preparation and Hybridization

Nick translation is a method for the introduction of the labeled nucleotides into a double-stranded DNA molecule by first making small nicks (Removal of a *phosphodiester bond* between two adjacent *nucleotides*) on one strand of the double stranded DNA with DNase, and then repairing with DNA polymerase I in the presence of labeled nucleotides. For Nick

translation the reaction master mix is made with respective BAC clones for each Hox cluster to get a the final total volume of 50ul.The components added are nuclease-free water, 5ul10X nick translation buffer (This is prepared with 0.5M Tris-HCL,50mM Magnesium chloride, 0.5mg/mLnuclease free BSA, pH7.8.), 5ul 0.1M DTT, 4uL d(GAC)TP mix (0.5mM dATP, 0.5mM dCTP, 0.5Mm dGTP),1uL 0.5mM dTTP, 6uL 0.5Mm aminolly –dUTP (This is prepared by diluting the aminoallyl-dUTP 4-fold in nuclease free water to a final concentration of 0.5 mM), 1uL DNA template 1ug/ul,5ul DNASE (this is prepared by diluting 1uL of the 1mg/mL DNase I stock solution into 1mL of cold 1X nick translation buffer and then left on ice.), 1.5uL DNA polymerase I, 10U/uL.It is incubated at 15degree Celsius for 30 minutes.DNA is purified using the Quagen kit.

Ares Reaction: We used Invitrogen ARES DNA labeling kits to label our nick translated probes by attaching specific fluorochromes by an amino reaction. We used 4 different fluorochromes for each Hox Cluster: Alexa flour488, 555, 564 and 647.

Slide preparation: The coverslip were taken from the ethanol container and dried overnight. They were incubated with poly-D-lysine for 15 min. Washed with PBS 3 times and dried overnight. The cells were trypsinised and plated into poly-D-lysine treated cover slips at a concentration 100X10 E-3 cells per slide. This was done by washing the slides with cells in PBS (37degees Celsius) for 3 times keeping them incubated 5 minutes for each wash. Fixation was achieved by incubation in 4% PFA at room temperature for 10 minutes.

Permeabilization: The cells were incubated in PBS with 0.5%TritonX-100 for 10 min and then incubated in 2mL of 20%glycerol in PBS for overnight. Cell permeabilization was achieved by submerging slides in liquid nitrogen for a few seconds until a characteristic “click” sound was heard. The slides were placed on a paper towel till the glycerol on the slide thawed.

This procedure was repeated three more times, while dipping the slide each time in glycerol. Then the slides were washed in 1XPBS three times for 5 minutes each and incubated in 0.1M HCL for 7 min. The slides were equilibrated in 50%formalydehyde with 2XSSC for two weeks at 4 degree Celsius to improve the hybridization efficiency. The fixed slides can be maintained for at least 2 weeks as it improvises the hybridization signals.

Probe Denaturation and Hybridization for 3D cells: DNA probe was dissolved in 12ul of hybridization buffer. The hybridization solution containing probe was added on each slide and slide and probe are simultaneously denatured for 4 minutes at 75 degrees Celsius. The cover slip was taken out of the six well plates and mounted on the each slide. It is then sealed with rubber cement, allowing it to dry completely and then placed on the hot plate at 74 degree Celsius for 4 min. Hybridization is done by placing the slide in an air tight, prewarmed humidified chamber and incubating for three days in the dark at 37 degrees Celsius. The post-hybridization washes involves washing the slide in for 30 minutes in 2XSSC in 37 degree Celsius and then washing them in 0.1X SSC for 30 minutes at 60 degree Celsius. Slides are counter stain with DAPI by incubating the slides in DAPI for 3 min and immediately mounting the slides using Gel mount.

Confocal multi-channel fluorescence microscopy was applied in order to dissociate signals from very small structures labeled with multiple fluorochromes with different excitation and emission wavelengths. Five colors (DAPI, Alexa 488, Alexa 555, Alexa 596, Alexa 647) labeled nuclei (Biomedia, refraction index=1.358$\pm$0.002) and examined under LSM510META (Zeiss, Thornwood, NY) microscope which is equipped with four laser sources (Blue diode 405 nm, Argon 488 nm, HeNe543 nm and HeNe633 nm). Multi-track acquisition was carefully configured to efficiently prevent possible bleed-through between fluorophores. No cross-talk was confirmed using color single controls. The pinholes for each photomultiplier/detector were

adjusted in x, y and z directions so that perfect alignment was achieved to minimize the chromatic aberration between ultraviolet, visible and infrared light wavelengths. To detect channel misregistration, multicolor microspheres (Focal Check, Invitrogen, and Molecular Probes) were imaged and any pixel shifts observed between channels were corrected in the sample images.

With Multi-Time, the automatic acquisition macro of LSM510, optical sections of approximately 30 nuclei were collected with water immersion 63x C Apochromat objective lens (N.A.=1.2) at zoom factor of 4 and Z-interval of 0.15m. The lens's correction collar was set to 0.17 to match the coverslip thickness. Using a micrometer, only cover slips measured correct thickness was used for cell culture. The pinholes for the each channel were individually adjusted to 1.0m optical slice according to the 543 nm detector pinhole set at one Airy Unit. Confocal 3-D data sets (512 x 512 x 40) were further cropped to one nucleus per image and processed with Huygens deconvolution program (Scientific Volume Imaging, Netherlands). Quick MLE (Maximum Likelihood Estimation) algorithm was applied for removal of noise and re-assigning of light signals to original structures. A Point spread function (PSF) was generated theoretically based on the microscopical parameters. Voxel (volume element for the pixel) size of images was 0.093 x 0.093 x 0.15 and met the sampling requirement of Nyquist theorem.

Section 5: SUMMARY

In this project we developed a cell model to investigate Hox gene nuclear architecture in ESC and their differentiated derivatives, NSC. Our results shows that FGF induced differentiation of ESC towards the neural lineage is correlated with the decreased expression of markers of cell pluripotentiality (Nanog) and the increase of NSC markers (Nestin), thus maintaining an appropriate trajectory of *in vivo* expression. We show for the first time that Hox gene expression is induced by FGF treatment in parallel of ESC differentiation towards the neural lineage. In NSC only the expression of members of the 5' Hox domain was detected, correlating with previous reports showing that this domain is sensitive to FGF pathway regulation.

We observe that nuclear volume and sphericity index changes as cells undergo differentiation and commit to neural lineage. This provides the base for our null hypothesis which states that reorganization of Hox clusters positions within the cells are proportional to the change in the nuclear shape of the cells as they get differentiated to NSC. As the nucleus gets elongated in NSC, a parallel change in the distances between the homologous clusters was expected. The analysis of the angular distribution of Hox cluster with respect the nuclear axis shows that homologous clusters get reoriented to adjust to the change in the shape of the nucleus that parallels cell differentiation. However, with the exception of Hox A, the interallelic distances between the other Hox genes are much conserved between cell types, thus rejecting our null hypothesis. Moreover, these results shows the strong conservation of the interallelic distances between in both cell types

Our results of radial distribution of Hox A, B and C gene clusters between ESC and NSC shows no significant difference between the two cell types with the exception of Hox D cluster

that shifts significantly towards the nuclear center in NSC. We can conclude from the angular distribution as well as the radial distribution that there is a change in the nuclear positions of Hox D cluster in NSC as compared to ESC. This is despite the fact that there is no significant change in the interallelic distances between the homologous pairs of Hox D.

It is interesting to note that on comparing the combined distances between all the clusters, we observe that homologous Hox genes physically associate (colocalize) in NSC and not in ESC. This may be related with genomic imprinting transcriptional regulation, which is more relevant in NSC where Hox genes are expressed. However we do not observe nuclear colocalization of Hox heterologous cluster (paralogs) either in ESC or in NSC, suggesting that collinear regulation of paralogs Hox genes is not a simple phenomenon of physical interaction of the paralog clusters. However, we must consider that physical association of the clusters may be a sporadic occurrence not detected in our sample size. To overcome this pitfall, we developed a mathematical model to map the position of Hox cluster by normalizing all nuclei to a common platform using “affine transformation”.The scatter plots after the affine transformation shows that for ESC, the Hox gene clusters are predominantly positioned towards the center in a top-down manner where as in NSC the Hox gene clusters are more scattered even though homologous clusters occupy similar domains.

Our preliminary data show that paralog Hox clusters tend to occupy a similar nuclear domain in NSC, which may facilitate long-range gene interaction.

Section 6: CONCLUSION

In overall, our results indicate that Hox gene cluster nuclear tridimensional organization is neither random nor correlated to the changes in nuclear volume and shape that parallel cell differentiation. The absence of colocalization between the heterologous Hox clusters in both cell types suggests that long range chromosomal interactions between Hox clusters are sporadic events. The small data sample size may have hindered the chances of any visible long range interaction. However, after analyzing the nuclear architecture on a comprehensive mathematical model we do see heterologous Hox clusters sharing common nuclear domains in NSC. This phenomenon hardly exits in ESC. After the affine transformation the Hox genes are seen to be predominantly positioned towards the center in ESC whereas they are scattered in NSC.

In spite of extensive research aimed to analyze the relationship between 3D nuclear architecture and genome function, we still do not have an accurate experimental design developed till date.A valid mathematical model must include various topographic landmarks, such as nucleolus, which may also help us to understand the functional implications of nuclear architecture. Mathematical modeling analysis must focus to quantify the frequency of occupancy of Hox clusters in their discrete nuclear domains and compare them with the analysis of the radial distribution or distances between loci. This form of modeling will provide a better understanding of the overall Hox cluster organization in the nucleus.

Section 7: Reference List

Bacher,C.P., Guggiari,M., Brors,B., Augui,S., Clerc,P., Avner,P., Eils,R., and Heard,E. (2006). Transient colocalization of X-inactivation centres accompanies the initiation of X inactivation. Nat. Cell Biol. *8*, 293-299.

Baylin,S.B. and Schuebel,K.E. (2007). Genomic biology: the epigenomic era opens. Nature *448*, 548-549.

Bel-Vialar,S., Itasaki,N., and Krumlauf,R. (2002). Initiating Hox gene expression: in the early chick neural tube differential sensitivity to FGF and RA signaling subdivides the HoxB genes in two distinct groups. Development *129*, 5103-5115.

Berger,A.B., Cabal,G.G., Fabre,E., Duong,T., Buc,H., Nehrbass,U., Olivo-Marin,J.C., Gadal,O., and Zimmer,C. (2008). High-resolution statistical mapping reveals gene territories in live yeast. Nat. Methods *5*, 1031-1037.

Bernstein,B.E., Kamal,M., Lindblad-Toh,K., Bekiranov,S., Bailey,D.K., Huebert,D.J., McMahon,S., Karlsson,E.K., Kulbokas,E.J., III, Gingeras,T.R., Schreiber,S.L., and Lander,E.S. (2005). Genomic maps and comparative analysis of histone modifications in human and mouse. Cell *120*, 169-181.

Bernstein,B.E., Meissner,A., and Lander,E.S. (2007). The mammalian epigenome. Cell *128*, 669-681.

Bickmore,W.A., Mahy,N.L., and Chambeyron,S. (2004). Do higher-order chromatin structure and nuclear reorganization play a role in regulating Hox gene expression during development? Cold Spring Harb. Symp. Quant. Biol. *69*, 251-257.

Blobel,G. (1985). Gene gating: a hypothesis. Proc. Natl. Acad. Sci. U. S. A *82*, 8527-8529.

Branco,M.R. and Pombo,A. (2006). Intermingling of chromosome territories in interphase suggests role in translocations and transcription-dependent associations. PLoS. Biol. *4*, e138.

Branco,M.R. and Pombo,A. (2007). Chromosome organization: new facts, new models. Trends Cell Biol. *17*, 127-134.

Brown,J.M., Leach,J., Reittie,J.E., Atzberger,A., Lee-Prudhoe,J., Wood,W.G., Higgs,D.R., Iborra,F.J., and Buckle,V.J. (2006). Coregulated human globin genes are frequently in spatial proximity when active. J. Cell Biol. *172*, 177-187.

Chambeyron,S. and Bickmore,W.A. (2004). Chromatin decondensation and nuclear reorganization of the HoxB locus upon induction of transcription. Genes Dev. *18*, 1119-1130.

Chiu,C.H., Amemiya,C., Dewar,K., Kim,C.B., Ruddle,F.H., and Wagner,G.P. (2002). Molecular evolution of the HoxA cluster in the three major gnathostome lineages. Proc. Natl. Acad. Sci. U. S. A *99*, 5492-5497.

Chubb,J.R., Boyle,S., Perry,P., and Bickmore,W.A. (2002). Chromatin motion is constrained by association with nuclear compartments in human cells. Curr. Biol. *12*, 439-445.

Conti,L., Pollard,S.M., Gorba,T., Reitano,E., Toselli,M., Biella,G., Sun,Y., Sanzone,S., Ying,Q.L., Cattaneo,E., and Smith,A. (2005). Niche-independent symmetrical self-renewal of a mammalian tissue stem cell. PLoS Biol. *3*, e283.

Cremer,T. and Cremer,C. (2001a). Chromosome territories, nuclear architecture and gene regulation in mammalian cells. Nat. Rev. Genet. *2*, 292-301.

Cremer,T. and Cremer,C. (2001b). Chromosome territories, nuclear architecture and gene regulation in mammalian cells. Nat. Rev. Genet. *2*, 292-301.

Cremer,T., Cremer,M., Dietzel,S., Muller,S., Solovei,I., and Fakan,S. (2006a). Chromosome territories--a functional nuclear landscape. Curr. Opin. Cell Biol. *18*, 307-316.

Cremer,T., Cremer,M., Dietzel,S., Muller,S., Solovei,I., and Fakan,S. (2006b). Chromosome territories--a functional nuclear landscape. Curr. Opin. Cell Biol. *18*, 307-316.

Deschamps,J. and van Nes,J. (2005). Developmental regulation of the Hox genes during axial morphogenesis in the mouse. Development *132*, 2931-2942.

Grewal,S.I. and Jia,S. (2007). Heterochromatin revisited. Nat. Rev. Genet. *8*, 35-46.

Hepperger,C., Mannes,A., Merz,J., Peters,J., and Dietzel,S. (2008). Three-dimensional positioning of genes in mouse cell nuclei. Chromosoma *117*, 535-551.

Huang,S., Li,X., Yusufzai,T.M., Qiu,Y., and Felsenfeld,G. (2007). USF1 recruits histone modification complexes and is critical for maintenance of a chromatin barrier. Mol Cell Biol. *27*, 7991-8002.

Lanctot,C., Kaspar,C., and Cremer,T. (2007). Positioning of the mouse Hox gene clusters in the nuclei of developing embryos and differentiating embryoid bodies. Experimental Cell Research *313*, 1449-1459.

Lehoczky,J.A., Williams,M.E., and Innis,J.W. (2004). Conserved expression domains for genes upstream and within the HoxA and HoxD clusters suggests a long-range enhancer existed before cluster duplication. Evol. Dev. *6*, 423-430.

Lewis,E.B. (1978a). A gene complex controlling segmentation in Drosophila. Nature *276*, 565-570.

Lewis,E.B. (1978b). A gene complex controlling segmentation in Drosophila. Nature *276*, 565-570.

Lomvardas,S., Barnea,G., Pisapia,D.J., Mendelsohn,M., Kirkland,J., and Axel,R. (2006). Interchromosomal interactions and olfactory receptor choice. Cell *126*, 403-413.

Marenduzzo,D., Micheletti,C., and Cook,P.R. (2006). Entropy-driven genome organization. Biophys. J. *90*, 3712-3721.

Meaburn,K.J., Misteli,T., and Soutoglou,E. (2007). Spatial genome organization in the formation of chromosomal translocations. Semin. Cancer Biol. *17*, 80-90.

Minton,A.P. (2005). Models for excluded volume interaction between an unfolded protein and rigid macromolecular cosolutes: macromolecular crowding and protein stability revisited. Biophys. J. *88*, 971-985.

Misteli,T. (2001a). The concept of self-organization in cellular architecture. J. Cell Biol. *155*, 181-185.

Misteli,T. (2001b). The concept of self-organization in cellular architecture. J. Cell Biol. *155*, 181-185.

Misteli,T. (2004). Spatial positioning; a new dimension in genome function. Cell *119*, 153-156.

Moon,H., Filippova,G., Loukinov,D., Pugacheva,E., Chen,Q., Smith,S.T., Munhall,A., Grewe,B., Bartkuhn,M., Arnold,R., Burke,L.J., Renkawitz-Pohl,R., Ohlsson,R., Zhou,J., Renkawitz,R., and Lobanenkov,V. (2005). CTCF is conserved from Drosophila to humans and confers enhancer blocking of the Fab-8 insulator. EMBO Rep. *6*, 165-170.

Ruault,M., Dubarry,M., and Taddei,A. (2008). Re-positioning genes to the nuclear envelope in mammalian cells: impact on transcription. Trends Genet. *24*, 574-581.

van,D.R., Fransz,P.F., and Verschure,P.J. (2003). The eukaryotic genome: a system regulated at different hierarchical levels. J. Cell Sci. *116*, 4067-4075.

Williams,R.R., Broad,S., Sheer,D., and Ragoussis,J. (2002). Subchromosomal positioning of the epidermal differentiation complex (EDC) in keratinocyte and lymphoblast interphase nuclei. Exp. Cell Res. *272*, 163-175.

Xu,N., Tsai,C.L., and Lee,J.T. (2006). Transient homologous chromosome pairing marks the onset of X inactivation. Science *311*, 1149-1152.